TREBALL FINAL DE MÀSTER

TÍTOL

RESIDUAL STRENGTH OF COMPACTED BOOM CLAY: DEPENDENCY ON STRESS, SUCTION AND MICROSTUCTURE.

AUTOR

MICHELLE C. PÉREZ CANALS

TUTOR

DR. JEAN VAUNAT

DR. ENRIQUE ROMERO MORALES

ESPECIALITAT

GEOTECHNICAL ENGINEERING

DATA

OCTOBER 22, 2013

Dept. d'Enginyeria del Terreny, Cartogràfica i Geofísica
E.T.S. Enginyers de Camins, Canals i Ports
UNIVERSITAT POLITÈCNICA DE CATALUNYA

Abstract

This investigation aims at studying the residual shear strength behavior of unsaturated Boom Clay from a microstructural viewpoint. The study focuses on statically compacted samples to simulate the in situ state of compacted clay. To study the microstructural aspects of compacted soils, an in depth literature review is conducted on the microstructure of compacted and remolded clays. Mercury intrusion porosimetry tests were carried out on selected samples of compacted Boom Clay and the results are compared with previous MIPS tests on compacted and remolded Boom Clay. The residual shear strength of compacted Boom Clay at very large strain is studied using a modified Bromhead ring shear apparatus designed and tests were performed on specimens prepared at different low target water contents and statically compacted. The test results were compared with previous tests on unsaturated Boom Clay by Merchán (2011) which had been prepared at higher water content and dried to the target suction under loaded conditions. Finally a definition of effective stress that includes microstructural features for compacted and remolded soils is proposed.

Resumen

Esta investigación propone estudiar el comportamiento en corte de Boom Clay en estado no saturado desde un punto de vista microestructural. El estudio se centra en muestras compactadas estáticamente para simular el estado in situ de arcillas compactadas. Para estudiar los aspectos microestructurales de suelos compactados, se llevó a cabo una investigación a fondo de la literatura disponible sobre la microestructura de arcillas compactadas y remoldadas. Varios ensayos de porosimetria de intrusión de mercurio se llevaron a cabo en algunas muestras de Boom Clay compactada y se los resultados se compararon con ensayos MIP realizados anteriormente en Boom Clay compactada y remoldada. La resistencia en corte a grandes deformaciones se estudió utilizando una modificación del equipo de corte anular Bromhead. Las muestras preparadas al contenido de humedad deseado fueron compactadas y ensayadas. Los resultados se compararon con los resultados obtenidos por Merchán (2011) en su tesis en muestras que habían sido preparadas con contenidos de humedad más altos y secados posteriormente para alcanzar la succión deseada. Finalmente se presenta una definición de tensión efectiva que incluye aspectos microestructurales para suelos compactados y remoldados.

Table of Contents

List of Figures

List of Tables

Notation

α: Shear strength parameter

b_w: Average slope of the wetting and drying branches water retention curve

d: Entrance pore size diameter

e: Void ratio

e_m: Micro void ratio

e_M: Macro void ratio

e_{free}: Free void ratio

Δe: Non-intruded void ratio

e_0: Initial void ratio

e_{int}: intruded void ratio

e_{ext}: Extruded void ratio

e_w: Total water ratio

e^*_m: The water ratio corresponding to saturated microstructure and dry macrostructure

ξ_m: Ratio of microvoid ratio to total void ratio

γ_d: Dry unit weight

G_s: Density of solid particles

p: Absolute pressure

φ_{res}: Residual internal friction angle

φ_{sat}: Residual internal friction angle corresponding to saturated state

φ'': Friction angle with respect to changes in suction

Ψ: Total suction

θ_{nw}: Contact angle between mercury and the pore wall

s: Matric suction

s_{max}: maximum suction corresponding to e_w

s^*_w: Suction corresponding to e^*_m

Sr: Degree of saturation

S_e: Effective degree of saturation

S_{rm}: Degree of saturation of the microstructure

S^*_{rm}: Degree of saturation for the saturated microstructure

σ_{Hg}: Surface tension of mercury

σ_v: Net normal stress

σ': Saturated effective stress

σ'': Unsaturated effective stress

σ'_m: Effective stress of the microstructure

σ'_M: Effective stress of the macrostructure

τ: Shear strength

τ_{res}: Residual shear strength

τ/σ_v: Normalized residual strength

u_w: Pore water pressure

u_a: Pore air pressure

w: Gravimetric water content

w^*: Gravimetric water content corresponding to saturated micropores

w_l: Liquid limit

w_p: Plastic limit

w_{res}: Gravimetric water content for residual state

χ: effective stress parameter (Bishop, 1959)

1. Introduction

Saturated soil mechanics has dominated the geotechnical engineering field since its beginning with the definition of effective stress by Terzaghi. However in the past decades, interest has grown in unsaturated soil mechanics with the identification of stress state variables to define unsaturated states, particularly in relation to compacted and residual soils. It has been shown that these stress state variables are more general and can include all the principles of saturated soil mechanics, like the Mohr-Coulomb shear strength criterion (Leong et al., 2001). The shear strength of soil is a fundamental aspect in many engineering applications including bearing capacity, slope stability, embankments, retaining walls and pavement subgrades. The importance of the residual strength of soils is well recognized in several geotechnical problems, such as reactivation of landslides, pile friction resistance, earthworks and so on. In most of this applications soil is found in unsaturated states and therefore further understanding of unsaturated shear strength behavior, particularly residual shear strength, is needed.

Recently Merchán (2011) presented experimental evidence of the increase in residual shear strength of Boom Clay at high total suctions. A significant increase in the internal friction angle of remolded samples was observed. This investigation is intended as a continuation of his thesis to further investigate the influence of microstructure in residual shear strength of Boom Clay at high suctions. Statically compacted samples prepared at target suctions will be studied with the same ring shear apparatus designed by Merchán. The investigation aims to provide an experimental basis for the definition of an effective stress that includes microstructural features for compacted and remolded soils.

1.1. Boom Clay

The soil used in the investigation was artificially prepared powder from natural Boom Clay proceeding from Belgium. Much research has been performed on the geotechnical characteristics of Boom Clay (Horsemann et al, 1987; Romero, 1999; Bernier et al,1997; Merchán, 2011) due to its proposed use as a host medium for geologic disposal of radioactive waste. For this reason extensive characterization and comprehensive information is available on this material in unsaturated states and therefore it was chosen for the investigation. Boom Clay is a tertiary formation which is the youngest argillaceous unit of a sequence of marine clays and sands deposited during the Middle Oligocene in the northern European sedimentary province (Horsemann et al, 1987). It is a medium plasticity clay with a composition of Kaolinite/Illite (50%), Smectite (5%) and Quartz and Feldspars (30-40%). The liquid limit is w_l=55±2%, plastic limit w_p=28±2% and density of solid particles is G_s=2.70 Mg/m3 (Romero 1999).

2. Microstructure of compacted clays

2.1. Clay and Structure

Clay structure plays an important role in the mechanical behavior, such as shear strength and tensile strength, of clayey soils. Clay is defined as naturally occurring material composed primarily of fine-grained minerals, which is generally plastic at appropriate water contents (Guggenheim et al, 1995). Clay minerals are hydrous silicates or alumino silicates and may be defined as those minerals which dominantly make up the colloidal fraction of soils, sediments, rocks and waters. Clays consist of a heterogeneous mixture of finely divided minerals, such as quartz, feldspars, calcite, etc. (Luckham and Rossi, 1999). These fine grained materials range from particles of clay minerals that have a crystal structure formed from a stack of layers interspaced with interlayers to aggregates formed from mineral particles which vary in size depending on water content. Aggregation is described by face to face (FF) association, and refers to the collapse of the diffuse double layers and the formation of aggregates of parallel platelets spaced 20 Å or less apart (Luckham and Rossi, 1999). At high water contents large aggregates are formed, on the other hand it has been observed that at very low water contents (w<10%) aggregate size does not differ much from aggregates formed at hygroscopic water content (Tarantino 2011).

The formation of clay particle aggregates give way to the double structure of clayey soils. This double structure supposes a double porosity that has been observed in compacted clay materials (Tarantino, 2011; Koliji et al., 2010; Romero, 2011; Lloret et al., 2003; Monroy et al., 2010). The structure of the aggregates is the microstructure and its porosity is referred to as micropores or intra-aggregate porosity. Whereas the arrangement of the aggregates is the macrostructure and the pores between aggregates are referred to as macropores or inter-aggregate porosity. Figure 2.1 present a schematic representation of the microfabric of a compacted clayey soil. The presence of both air and water in the soil affects the evolution of the multimodal pore network. Studies have illustrated that the microstructure of a given compacted soil is not unique and strongly depends on the preparation method used and on the paths followed to reach a given point in the compaction plot (Koliji et al., 2010; Tarantino and Col, 2008; Vanapalli et al., 1999; Griffiths and Joshi, 1989; Sivakumar and Wheeler, 2000). The macropores are strongly affected by the loading process, while the micropores are primarily affected by changes in the water content (Romero, 2011).

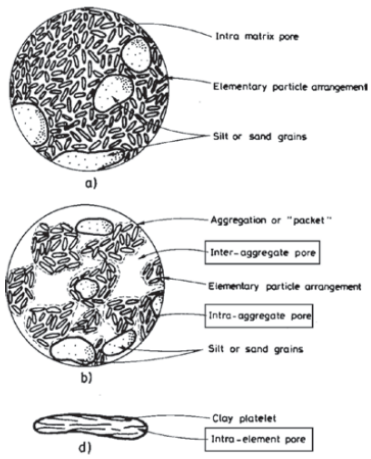

Figure 2.1 Inter-aggregate, intra-aggregate and intradomain (intra-element) pores in clayey soils. a) compacted on the wet side of optimum. b) compacted on the dry side of optimum. d) elementary particle arrangement of domain (Tarantino, 2011)

Water present in clayey soils can be found in four different forms as described by Hueckel (1992). First bulk water which is the free water or capillary water found in the macropores, it is able to flow due to hydraulic gradient. Second intercluster adsorbed water which envelopes clusters of smectite, illite and single particles and fills the intra aggregate pores. This water is restricted from flow in normal conditions. Third intracluster adsorbed water associated with interlamellar surfaces in smectites. Finally structural water or hydroxyl which is part of the structural lattice of the clay mineral. The soil water interaction is important in clay structure, the structure is dependent of water that interacts within the clay layers and within the aggregate particles (Saiyouri et al., 2000). Bulk water and intercluster water are the main interest in this study.

Wetting and drying cycles have an effect on clay structure causing a rearrangement of particles and inducing particle aggregation even after a first cycle causing a reduction in the swelling potential of the soil with various cycles (Al-Homoud et al., 1995). Irreversible volume changes during cycles have been observed (Wheeler et al., 2003), however after a few cycles a more stable structural arrangement is achieved causing a nearly reversible volumetric condition. It is also noted that total volumetric deformations accumulated at the end of a cycles increase exponentially with applied vertical stress, at low vertical net stress reversible volumetric behavior is observed from the first cycle (Farulla et al., 2010).

Drying or desaturation of soil is of great interest for the study. Vanapalli et al. (1999) presents three stages of desaturation for soils. The boundary effect stage when almost all pores are filled with water. The transition stage which is when the soils begins to de-saturate because the air entry value has been reached and the soil dries rapidly with increasing suction. Finally the residual stage is when a degree of saturation has been reached in which the liquid phase becomes discontinuous. In this stage large increases in suction

lead to small changes in degree of saturation. The samples used in this study are mostly in the residual stage of saturation. The drying characteristics of soils prepared in the wet of optimum is controlled by the microstructure whereas soils prepared on the dry of optimum it is controlled by the macrostructure because of the large pores between aggregates.

2.2. Water retention properties of Boom Clay

Water retention properties of Boom Clay are of importance in establishing its behavior in unsaturated states. The water retention curve determines the relationship between water content or degree of saturation of the soil with the total suction. The curve can be divided into two parts, when water is contained within the aggregates (high suction range), and when water begins to fill the pores between the aggregates (low suction range). For Boom Clay the value of gravimetric water content for the delimiting point in the retention curve between intra- and inter-aggregate governing suction corresponds to *w*= 13-15%, at very high density packing the value may be lower (Romero et al.,1999; Merchán 2011). The low suction range is affected by soil dry density; loading mechanisms reduce the macroporosity affecting bulk water and causing soils with the same gravimetric water content have different suction (Romero et al., 1999). At low water contents or high suction range the influence of soil density is negligible and the retention curve depends on the mineralogical composition of the clay and its specific surface. In the high suction range gravimetric water content is a more adequate state variable for the retention curve than degree of saturation.

This study concentrates on Boom Clay compacted in the high suction range. Total suction was determined for samples that were later tested in the ring shear device. A Psychrometer (WP4 dew-point mirror psychrometer) was used to measure total suction. The suction measurements were compared with measurements made on Boom Clay by Romero et al. (1999). A model for the main wetting and drying branches of the water retention curve proposed by Romero et al. (2011) is presented in equation 2.1. It accounts for the swelling and shrinkage of the aggregates induced by water content change. It describes the micro and macropore retention mechanisms separately. The equation proposed for the high suction range was used in this study. It accounts for the water stored in the micropores and does not depend on the void ratio as has been observed at high suction (Bernier et al., 1997; Romero et al., 1999; Romero and Vaunat, 2000; Tarantino and De Col, 2008; Tarantino, 2011).

$$e_{wD,W} = \frac{b_{D,W} e_m^*}{ln\left(\frac{s_{max}}{s_{mD,W}^*}\right)} \left[\frac{b_{D,W} + ln\left(\frac{s_{max}}{s_{mD,W}^*}\right)}{b_{D,W} + ln\left(\frac{s}{s_{mD,W}^*}\right)} - 1 \right] \tag{2.1}$$

$$e_w = \frac{V_w}{V_s} = wG_s \tag{2.2}$$

Equation 2.2 presents the total water ratio defined as the total volume of water by the volume of solids. The water ratio that corresponds to a saturated microstructure and a dry macrostructure is e^*_m. The equation defined in 2.1 is valid only for values of $e_w \leq e^*_m$. In equation 2.1, s^*_w is the suction corresponding to e^*_m, s_{max} is the maximum suction corresponding to e_w=0, b is the average slope of the branches and subscripts D and W refer to the parameters for each of the wetting and drying branches. In the absence of specific data Romero et al. (2011) suggests a value of s_{max} = 1 GPa. The parameters used for equation 2.1 are summarized in Table 2.2 and were taken from the calibration done by Della Vecchia et al. (2012).

Table 2.2Retention parameters for compacted Boom Clay in the high suction range (Della Vecchia et al., 2012).

e^*_m	b_D	s^*_{mD}	b_W	s^*_{mW}	s_{max}
0.38	6.5	6.7	12	2.4	1000

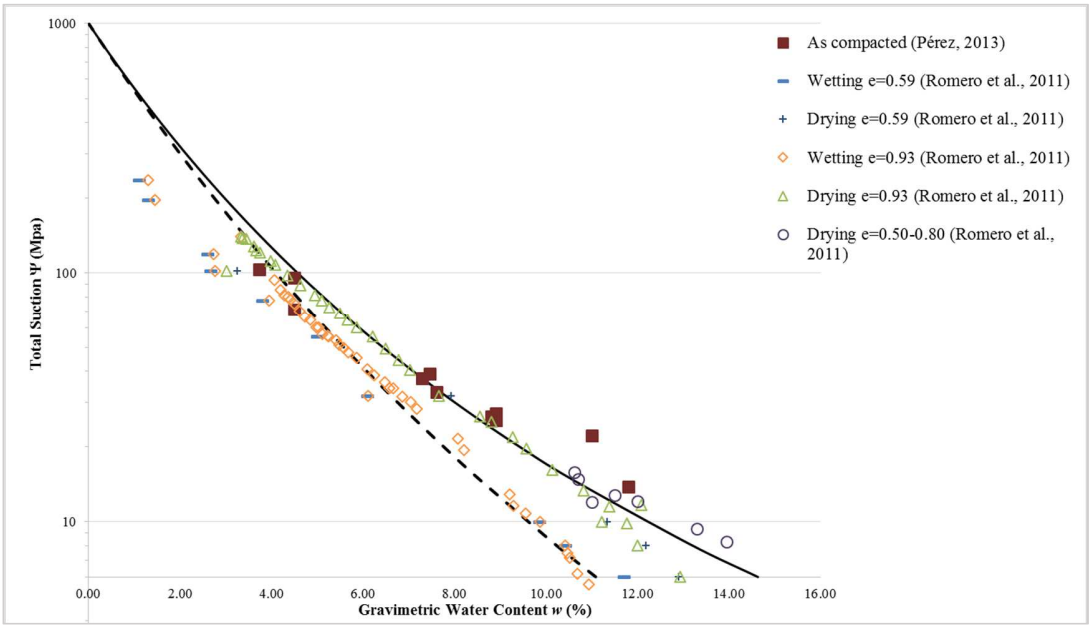

Figure 2.2 Comparison between the experimental data and model predictions for water retention curve of compacted Boom Clay.

Figure 2.2 presents the relationship between suction and water content for different compacted samples superimposed with the retention curves obtained from the model and drying and wetting of samples presented by Romero et al. (2011). The specimens used had void ratios ranging between 0.50-0.93, the void ratio seems to have no influence on the water retention properties as is expected for high suction ranges. It is observed that most samples lie within the drying path of the water retention curve. This indicates that soils compacted at very low water contents could be considered to be nearly on a drying path, and thus the total suction could be predicted when the compaction water content is known. From the observations it was

determined that the drying branch of the model is adequate to predict the suction of specimens in which the total suction was not measured.

2.3. Previous works on suction effects and microstructure of Boom Clay

The microstructure of Boom Clay and its relationship with mechanical hydraulic behavior in unsaturated states has been characterized in many studies. Romero (1999) studied the microstructure through Mercury Intrusion Porosimetry (MIPS) and Scanning Electron Microscope (SEM) at different dry unit weight corresponding to γ_d=13.7kN/m^3 and 16.7 kN/m^3 and w=15%. The resulting photomicrographs are presented in Figure . The double structure is observed with clay aggregates composed of clay platelets separated by a porous network at inter-aggregate level. The microporosity is similar in both samples as a result of having the same water content. Conversely the macroporosity is proven to be affected by the increasing compaction pressure. The 13.7 kN/m^3 sample shows clearly defined macropores while the 16.7kN/m3 sample shows some fused aggregates due to the collapsed inter-aggregate pores. SEM results corresponded with MIP results that will be presented in section 2.5.

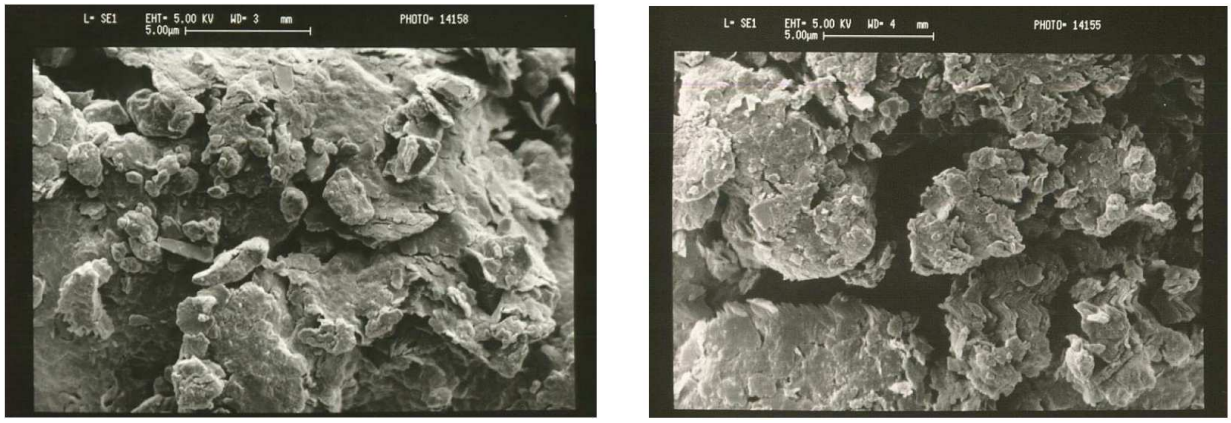

Figure 2.3 SEM photomicrograph for Boom Clay at different dry side compacted packing (x5000) (a) 16.7kN/m^3 (b)13.7 kN/m^3 (Romero, 1999).

Bernier et al. (1997) studied the swelling behavior of Boom Clay to validate the model for unsaturated expansive clays developed by Gens and Alonso (1992). They used Boom Clay prepared in two ways, as highly compacted pellets surrounded by clay powder and compacted clay. The tests performed were suction controlled oedometer tests at constant vertical stress and at constant volume. As predicted by the model the swelling produced by reducing suction decreases with increasing vertical stress until reaching a value where it collapses without swelling; and swelling pressure increases in a logarithmic relationship as suction

decreases. The double layer theory of the model was determined to be adequate for describing the swelling behavior.

The microstructure along with permeability and water retention of Boom Clay was studied by Romero et al. (1999). The intra aggregate pore water can be determined from MIP data, water retention curves and relative permeability tests. A delimiting value for pore diameter of the micro and macro porosity between d= 130-180 nm is proposed and a corresponding gravimetric water content for saturated micropores is w=15% from MIP data and w=13% from relative permeability tests. It was observed that the intra-aggregate porosity is not affected by mechanical effort, loading mechanisms on low water contents affects mainly the macroporosity that does not contain bulk water.

Suction effects and the relationship between suction and in situ stress states on intact Boom Clay block samples from great depth were investigated by Delage et al. (2007). Water retention properties and swelling properties of intact samples were investigated. Intact samples show greater water retention than compacted samples when compared to Romero et al. (1999) and Bernier et al. (1997). The relationship between suction of the saturated intact sample and in situ state of stress was also studied and found to be appropriate. Oedometer tests were performed to study the relationship between suction and loading and unloading. At low suction values, total suction is reduced with loading and increased with unloading reaching higher values of suction during the unloading.

2.4. Microstructure of remolded and compacted clay

It has been stated that the microstructure of clay is of importance in defining its mechanical properties in unsaturated states. Two significant types of microstructure are those presented by compacted soils, which present a double structure resulting from the formation of aggregates, and reconstituted or remolded soils which present a single porosity structure. Tarantino (2011) investigated in depth the microstructural properties of compacted and reconstituted soils focusing on the macroscopic behavior to determine the differences and similarities a review of the investigation along with other investigations is presented in this section.

Compacted clayey soils are characterized by a double porosity structure resulting from the aggregates formed when water is added to achieve a specific water content. The size of the aggregates vary with the water content, aggregation at low water contents is small since the aggregates are in unsaturated state while at water contents close to saturation the aggregates are very large. When aggregates are placed in a mold for compaction the inter aggregate pores are filled with air, as the soil is loaded the aggregates are subjected to undrained loading causing the pore water pressure inside the aggregates to increase, if the pore pressure becomes positive, water is expelled from the aggregates into the macropores. However if the aggregates

are in an unsaturated state, no water will be expelled and the macropores will remain dry. MIPS performed on clayey soils compacted on the dry side of optimum show a bimodal pore distribution characterized by a large amount of macropores while tests performed on wet of optimum and optimum samples show a monomodal distribution representing inter-aggregate pores. A simple microstructural model is presented Figure 2.4 by Tarantino (2011) to explain the transition from bimodal to monomodal distribution of pores in clayey soils. When water content is low, aggregates are small and inter aggregate pores are well defined but as water content increases the aggregates become larger and the inter-aggregate pores are reduced; through this mechanism it is suggested that the intra-aggregate pores of compacted soils are controlled by the compaction water content. Also aggregation created on compaction on the dry side of optimum is a permanent feature for the compacted soil fabric and the swelling and shrinkage of aggregates can be assumed as a reversible process in terms of water content (Romero, 2013).

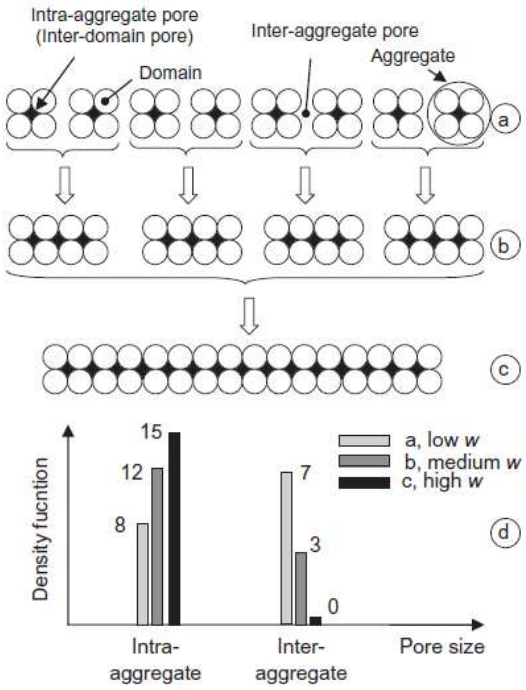

Figure 2.4 Schematic representation of the relationship between compaction water content and volume of intra-and inter-aggregate pores (Tarantino, 2011).

Investigations have shown that the size and frequency of inter-aggregate pores is controlled by the compaction effort (Tarantino, 2011; Lloret et al., 2013; Romero, 2013; Koliji et al., 2010). It has also been observed that at high water contents, when the microstructure is saturated, high compaction efforts have an effect on suction. As the degree of saturation is increased at constant water content by the compaction process, post-compaction suction increases at higher water contents, decreases at medium water content,

and remains constant at lower water contents (Tarantino and Col, 2008).The compaction method does not influence the final microstructure of compacted soils.

A comparison between MIPS and ESEM results of compacted and reconstituted soils at different suction and vertical loads was done by Koliji et al. (2010). The tests were done on a low plasticity clay prepared in a dry aggregate form that would be compacted and brought to the desired suction and in remolded samples that would also be brought to a desired suction. From the results it was observed that unsaturated aggregated samples exhibit a bimodal pore size distribution while remolded samples in the same conditions show a monomodal distribution with dominant pore radius being the same as the micropores in the aggregated sample. In reconstituted soils the intra and inter aggregate porosity are not easily distinguishable because inter-aggregate pores become of the same order of magnitude as the micropores. This effect is further enhanced by loading causing the macropores to collapse. Tarantino (2011) proposes that soil aggregates appear to be made of soil in reconstituted state

2.5. MIP on compacted clay

Mercury intrusion porosimetry has been used for the characterization of the microstructure of the compacted Boom Clay used in this study and compared to MIP results obtained by Merchán (2011). MIP is a technique in which a non-wetting liquid (mercury) is intruded at high pressure into a material sample to determine the size and distribution of its pores. For the technique the pores are assumed to be cylindrical and the relationship between the pressure used for intrusion and the pore diameter is given by the Washburn equation.

$$p = -\frac{4\sigma_{Hg}cos\theta_{nw}}{d} \qquad \text{(eq. 2.3)}$$

Where p is the absolute mercury pressure, σ_{Hg} is the surface tension of mercury (σ_{Hg}=0.484 N/m at 25^{o}C), and d is the entrance pore diameter. θ_{nw} is the contact angle between mercury and the pore wall, for Boom Clay it has a value of 140^{o} (Romero et al., 1999).

The limitations of MIP are: 1) Sample perturbation during freeze drying and mercury injection; 2) Enclosed porosity is not measured; 3) Constricted porosity is not detected until smaller pores are penetrated at higher pressures; 4) The smallest pores of the sample may be too small for the apparatus to intrude creating the non-intruded porosity; and 5) the minimum pressure of the apparatus limits the maximum pore size that can be detected (Romero and Simms, 2008; Simms & Yanful, 2004). For these reasons the void ratio detected by MIP tests does not correspond exactly with the calculated void ratio of the sample.

Samples tested on MIP apparatus have to be dry for the mercury to be able to intrude all the pores. The preferred method for drying the samples is freeze drying. Oven drying has been proven to cause significant

volume change and therefore it is not appropriate for correctly characterizing the microstructure of soils. Freeze drying is a process by which the material is frozen and the surrounding pressure is reduced allowing the frozen water to sublimate directly from the solid phase to the gas phase. Good results are obtained if the freezing is done quickly to avoid the formation of water crystals that could cause an increase in the water volume (Romero, 1999).

MIP tests were done using Micrometrics' AutoPore IV. The samples were prepared at three different target water contents corresponding to w = 3%, 5% and 10%. The Boom Clay powder was sprayed with demineralized water to achieve the desired water content and then passed through a No. 10 ASTM sieve to break down the large aggregates formed due to uneven wetting. The prepared soil was place in metallic bowls sealed with plastic and placed in the humidity chamber for at least 24h. A high density with a void ratio of e=0.55 was chosen because the soil samples were on a dry state and lower densities would not maintain the compaction density during the sample preparation. The three samples were placed in a static compaction mold and were compacted to the target density. Afterwards 1x1x1 cm^3 cubes were trimmed and freeze dried.

To have a wider view of the microstructure of compacted clay, MIP tests performed by Merchán (2011) and Romero (1999) were included for comparison. Figure 2.5 presents the range of void ratios and water contents included and Table 2.2 presents the initial values for the samples.

Table 2.2 Initial state of compacted samples for MIP tests

Sample	e	w	Sr
M1	0.54	0.035	0.18
M2	0.55	0.052	0.26
M3	0.49	0.104	0.57
M4*	0.93	0.32	0.93
M5*	0.65	0.22	0.91
M6*	0.49	0.17	0.94
M7*	0.54	0.165	0.83
M8*	0.93	0.258	0.75
M9*	0.84	0.243	0.78
M10*	0.71	0.214	0.81
M11*	0.6	0.178	0.80
M12*	0.48	0.11	0.62
M13*	0.57	0.064	0.30
M14*	0.71	0.079	0.30
M15°	0.59	0.15	0.69
M16°	0.93	0.15	0.44

*Merchán 2011

°Romero 1999

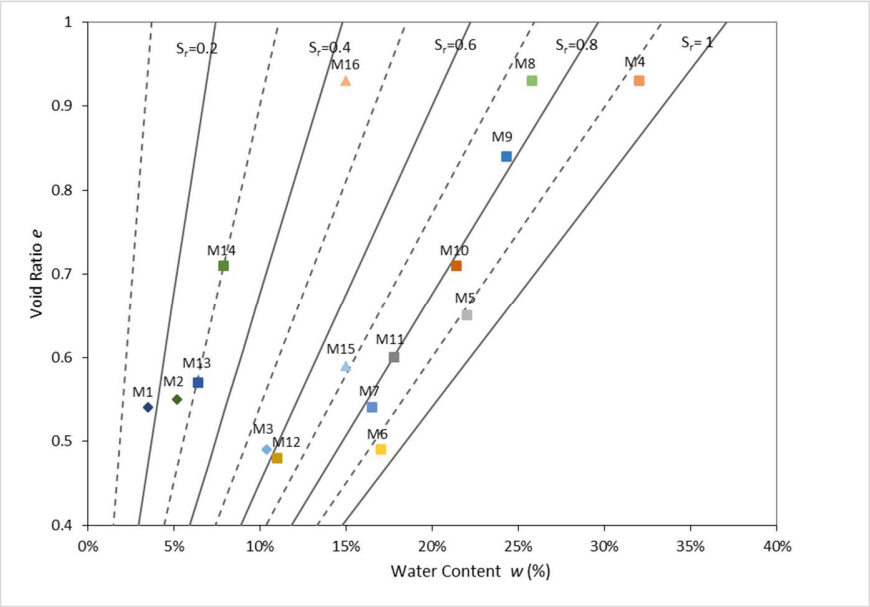

Figure 2.5 Statically compacted samples for MIP tests

Figure 2.6 to Figure 2.8 show the cumulative intrusion curve for samples M1, M2 and M3. The void ratio is similar for M1 and M2 while M3 has a slightly lower void ratio. To analyze the curves four parameters can be determined.

- Intruded void ratio e_{int}: Maximum void ratio of the cumulative intrusion curve.
- Extruded void ratio e_{ext}: Minimum void ratio of the extrusion branch.
- Non-intruded void ratio Δe: Enclosed porosity or pores that are too small to be intruded by the apparatus e_0-e_{int}.
- Free void ratio e_{free}: Non constricted porosity e_{int}-e_{ext}.

To determine the micro and macro void ratio the criteria proposed by Delage and Lefevbre (1984) based on the data from the intrusion/extrusion cycle was used. It proposes that the first intrusion fills all interconnected pore spaces and in the extrusion path only small pores are desaturated. A second mercury intrusion would follow the extrusion path demonstrating that large pores still remain fully saturated and are constricted by the smaller pores. Therefore e_{ext} can be defined as the void ratio corresponding to the macro-porosity e_M. Void ratio corresponding to the microporosity e_m can be defined as follows.

$$e = e_m + e_M \tag{2.4}$$

$$e_m = e_{free} + \Delta e \tag{2.5}$$

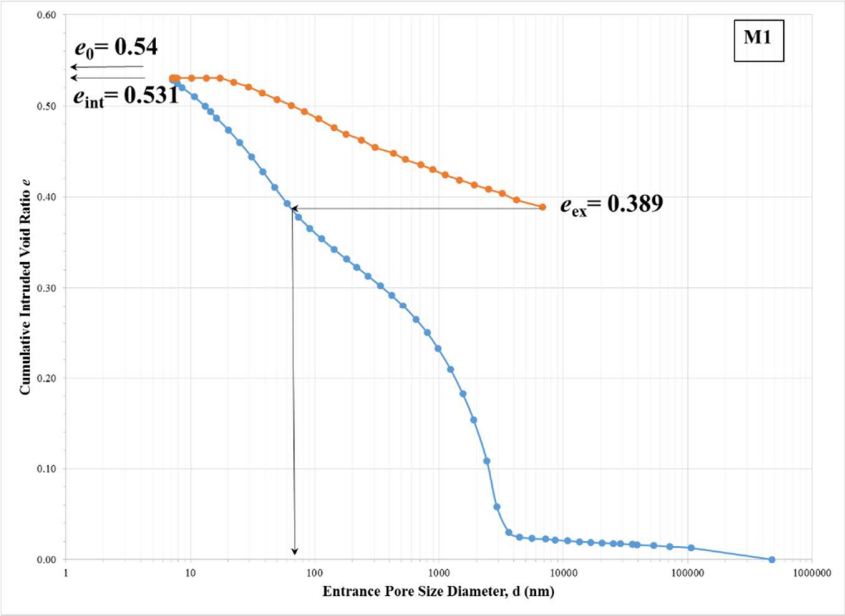

Figure 2.6 Cumulative intruded void ratio curve for M1

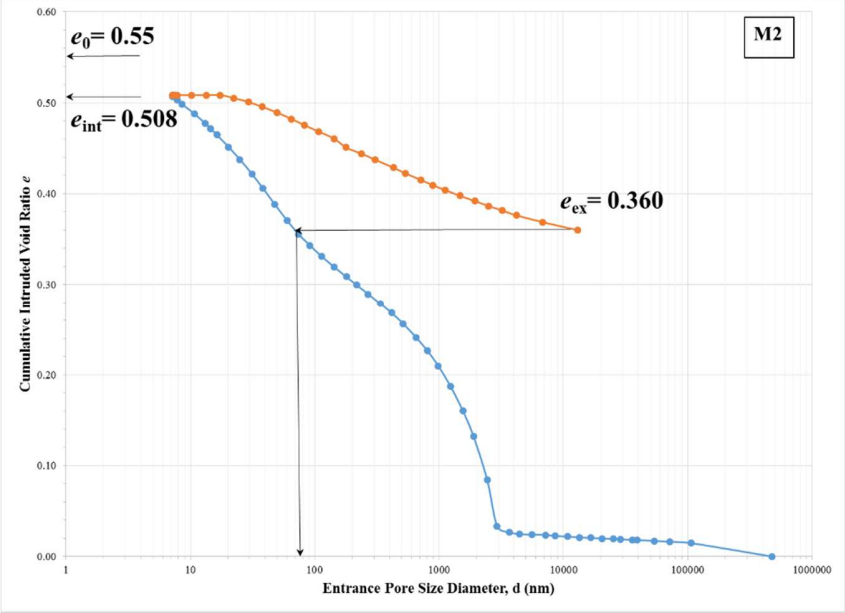

Figure 2.7 Cumulative intruded void ratio curve for M2

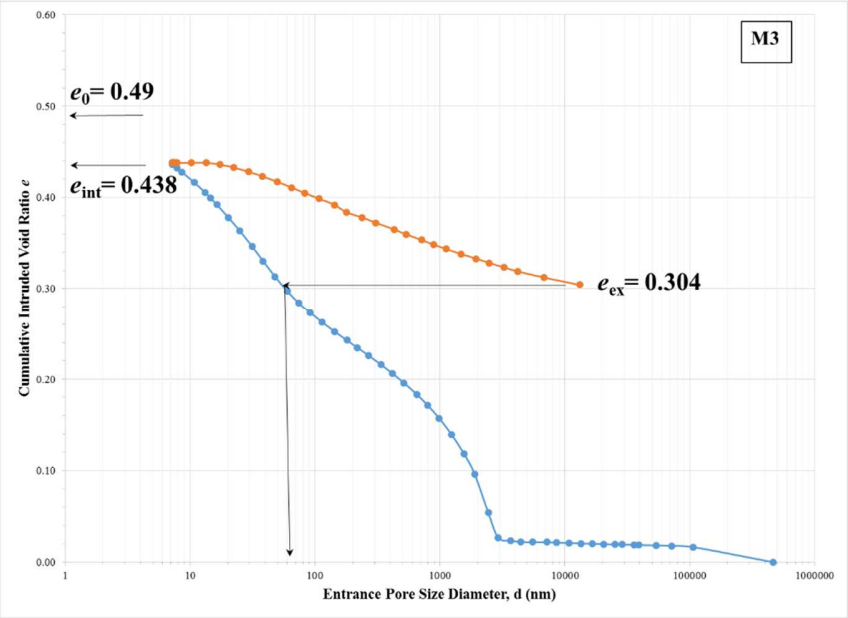

Figure 2.8 Cumulative intruded void ratio curve for M3

Using the extruded void ratio value from the cumulative intrusion curves, a delimiting size for pore diameter can be determined. The delimiting size for the microporosity is d=70 nm which is in accordance with the delimiting value found by Merchán (2011) for high density packings. Figure 2.9 presents the pores size distribution (PSD) curves for samples M1, M2 and M3. The specific water volume was calculated in equation 2.4.

The pore space occupied by water was determined in the PSD curve following the method proposed by Tarantino (2011). It is assumed that water saturates the smallest pores, and thus the pore diameter size separating the pores filled with water from those filled with air can be obtained by drawing a line at the difference between total void ratio and specific water volume on the cumulative intrusion curve and its intersection with the intrusion branch. It is observed in Figure 2.9 that for water contents of w=3% and 5% the aggregates remain unsaturated and at w=10% the microstructure is already saturated. The gravimetric water content for a fully saturated microstructure for Boom Clay had been determined to be higher w=12%-15% (Merchán, 2011; Romero et al., 1999). The PSD curve show no change in inter-aggregate porosity between the samples M1, M2 and M3 as is expected when the inter-aggregate pores are not saturated confirming that compaction water content controls the macropores. The macro porosity for M1 and M2 are very similar because the total void ratio is almost the same, on the other hand M3 has a void ratio of e=0.49 and has less macroporosity confirming that compaction density is reached at the expense of the inter-

aggregate pores. To further visualize the evolution of micro and macro void ratio and the specific water content Figure 2.10 presents graphically this relationship.

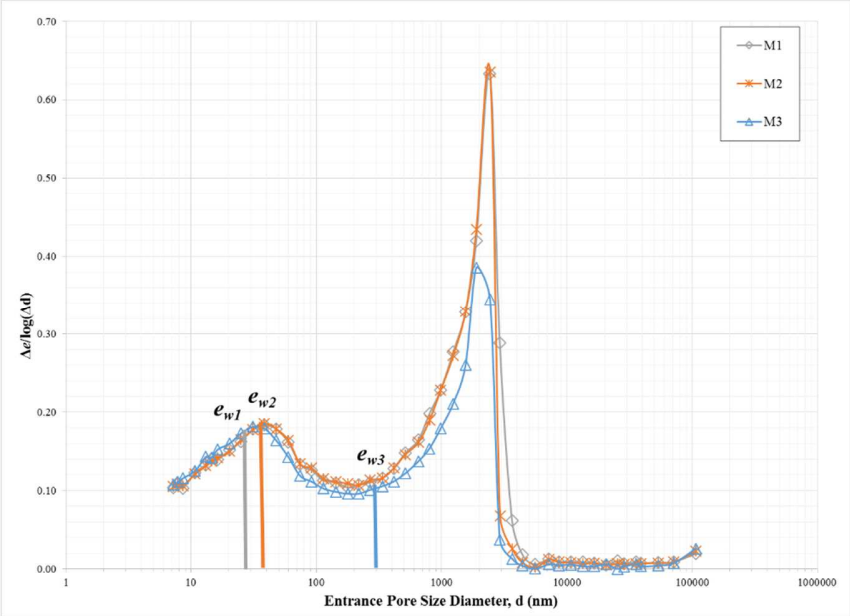

Figure 2.9 PSD curve for samples M1, M2 and M3

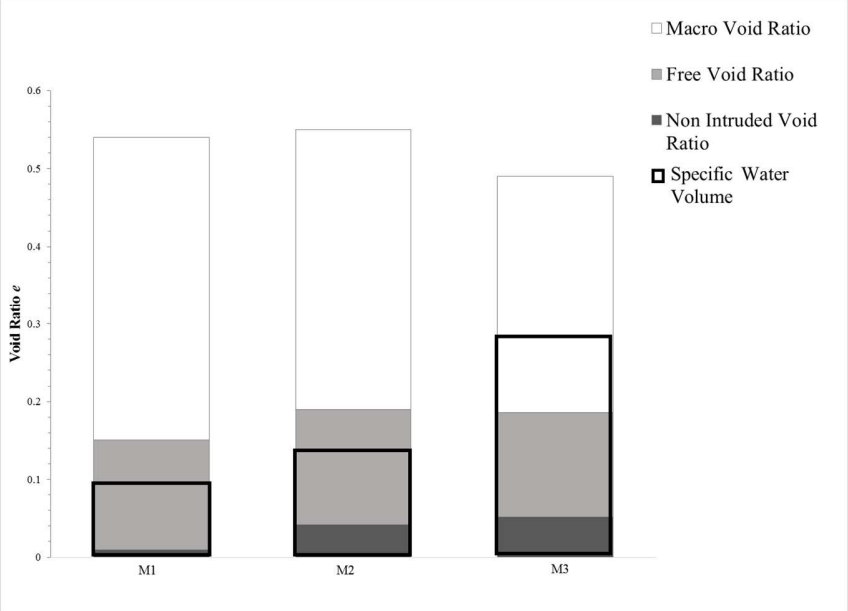

Figure 2.10 Distribution of micro and macro void ratio and specific water content

Figure 2.11 to Figure 2.13 present the PSD curves for samples tested by Merchán (2011). Figure 2.11 presents wet zone samples, the curves show a monomodal distribution with the majority of the pores within what is considered micropores. Upon analyzing the amount of micro and macro void ratio calculated for each sample it is evident that macro voids are present but their size is significantly reduced by the swelling of the micro pores. Also the micro void ratio reduces with the gravimetric water content. Figure 2.12 and Figure 2.13 present dry zone samples which present a clear bimodal distribution. Figure 2.12 presents samples with a fully saturated microstructure, and as is expected, the density of micropores increases with increasing water content and macropores decrease. Finally Figure 2.13 presents samples with an unsaturated microstructure similar to the samples used in this investigation. The pore distribution is in agreement with the distribution of Figure 2.9. Sample M12 has very similar properties to sample M3 and again the PSD curves are in agreement. Table 2.3 presents a summary of the values of micro void ratio and specific water content for samples tested in the investigation as well as samples from Merchán (2011) and Romero (1999).

To study the effect of drying on compacted soils, Merchán (2011) tested a sample initially prepared like M4 and left to air dry up to a value of e=0.46 and w=5.3%. The dried sample presented a monomodal pores size distribution similar to that of M4 but with a shift of dominant pore size diameter from 230nm to 52nm. The shrinking is observed in both the macro void ratio and the micro void ratio, achieving a micro void ratio similar to samples prepared on the dry side but a much smaller size of macro voids. Table 2.4 presents the values of micro void ratio and specific water content for comparison.

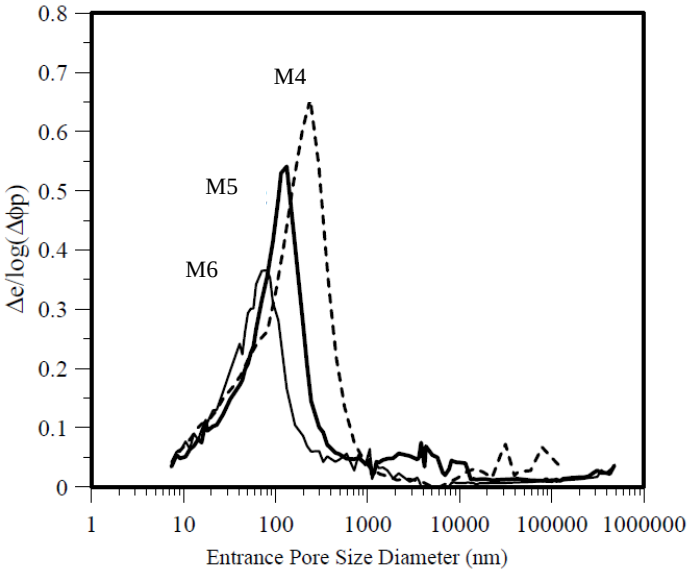

Figure 2.11 PSD curves for samples with Sr>0.90 (Merchán, 2011)

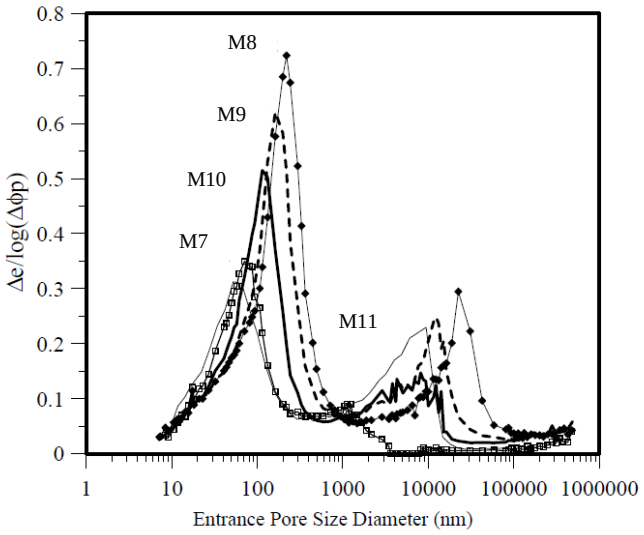

Figure 2.12 PSD curves for samples with Sr<0.84 (Merchán, 2011)

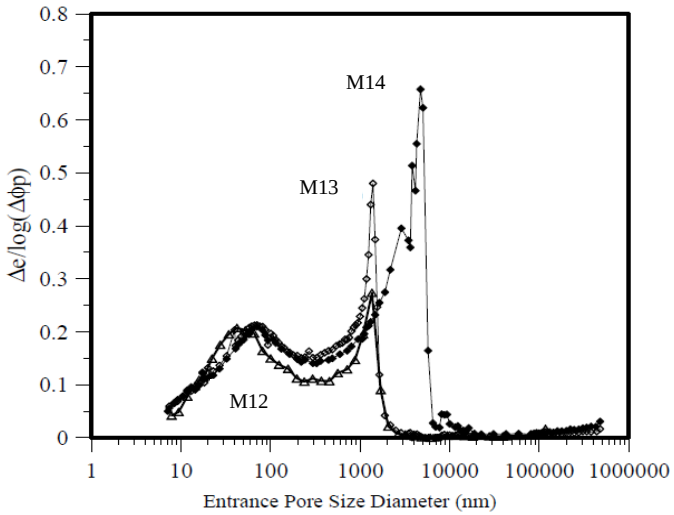

Figure 2.13 PSD curves for samples with Sr<0.70 (Merchán, 2011)

Table 2.3 Micro void ratio and specific water content for MIP tests on compacted samples

SAMPLE	e_0	w_0	S_r	e_{int}	Δe	e_{ex}	e_{free}	e_m	e_w
M1	0.54	0.035	0.18	0.53	0.01	0.389	0.141	0.151	0.095
M2	0.55	0.052	0.26	0.508	0.042	0.36	0.148	0.19	0.140
M3	0.49	0.104	0.57	0.438	0.052	0.304	0.134	0.186	0.281
M4*	0.93	0.32	0.91	0.766	0.164	0.493	0.292	0.437	0.864
M5*	0.65	0.22	0.92	0.467	0.18	0.283	0.184	0.362	0.593
M6*	0.49	0.17	0.93	0.335	0.16	0.179	0.156	0.313	0.457
M7*	0.54	0.165	0.82	0.346	0.19	0.212	0.134	0.329	0.44
M8*	0.93	0.258	0.75	0.752	0.17	0.579	0.173	0.348	0.7
M9*	0.84	0.243	0.78	0.671	0.17	0.512	0.159	0.33	0.66
M10*	0.71	0.214	0.82	0.533	0.17	0.375	0.158	0.333	0.58
M11*	0.6	0.178	0.8	0.439	0.161	0.304	0.135	0.3	0.48
M12*	0.48	0.11	0.62	0.357	0.123	0.283	0.074	0.197	0.3
M13*	0.57	0.064	0.3	0.421	0.149	0.245	0.176	0.325	0.17
M14*	0.71	0.079	0.3	0.616	0.094	0.476	0.14	0.234	0.21
M15°	0.59	0.15	0.69	0.515	0.0748	0.19	0.33	0.4	0.41
M16°	0.93	0.15	0.44	0.852	0.078	0.52	0.34	0.415	0.41

*Merchán 2011

°Romero 1999

Table 2.4 Micro void ratio and specific water content for MIP tests dried sample (Merchán, 2011)

SAMPLE	e_0	w_0	S_r	e_{int}	Δe	e_{ex}	e_{free}	e_m	e_w
Initial state	0.93	0.32	0.91	0.766	0.164	0.493	0.292	0.437	0.86
After drying	0.46	0.053	0.31	0.258	0.2	0.184	0.07	0.276	0.14

2.6. MIPS on remolded samples

MIP tests on remolded samples performed by Merchán (2011) will be used for comparison. The tests were performed on samples prepared at water contents between the plastic limit and liquid limit. Table 2.5 presents the initial and final conditions of the samples. Drying on samples was performed by placing on the ring shear apparatus and applying the vapor transfer technique. Samples R1 and R2 were prepared with the same conditions to verify the performance of the MIP device. The PSD curve for both samples showed to be similar.

Figure 2.14 presents the PSD curves of remolded samples compared with the PSD of compacted samples M4 M5 and M6. The remolded samples show a monomodal curve as is expected with main pore size diameter ranging between 200nm and 300nm. Some macroporosity is detected which is associated with the porosity between aggregates that were not completely fused. When compared with compacted samples

prepared at *Sr*>90 it is evident that the pore distribution is similar independently of the preparation path followed.

The drying PSD curves of the remolded samples compared with the compacted air dried sample are presented in Figure 2.15. Remolded samples present a shift to the left in the pore size distribution as well as a diminution in void density with respect to the original state. When compared with the compacted air dried sample, the PSD curves are very similar and the dominant pore size is the same. As mentioned in previous sections, even though remolded samples show a monomodal distribution, macro and micro pores can be distinguished. Drying of remolded samples is associated with some reduction in microporosity, but it was observed that macro porosity is more affected by the drying process.

Table 2.5 Initial and final conditions for MIP samples (Merchán, 2011)

Sample	e_0	w_0	Sr_0	e	w	Sr
R1	0.76	0.28	0.99	0.76	0.28	0.99
R2	0.76	0.28	0.99	0.76	0.28	0.99
R3	0.92	0.31	0.9	0.83	0.31	1.00
R4	1.00	0.37	1.00	0.62	0.067	0.29
R5	0.77	0.28	0.98	0.55	0.064	0.31
R6	0.95	0.33	0.92	0.81	0.3	1.00
R7	0.95	0.33	0.92	0.54	0.11	0.55

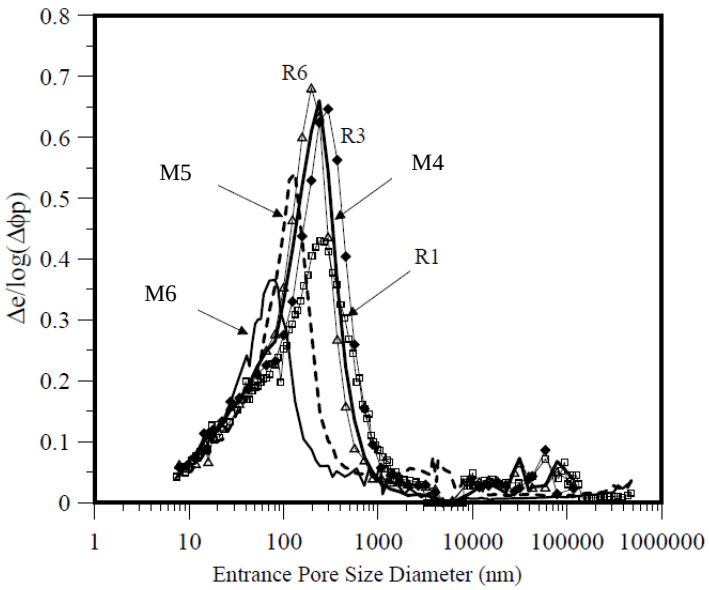

Figure 2.14 PSD curves for initial state remolded samples compared with wet side compacted samples (Merchán, 2011)

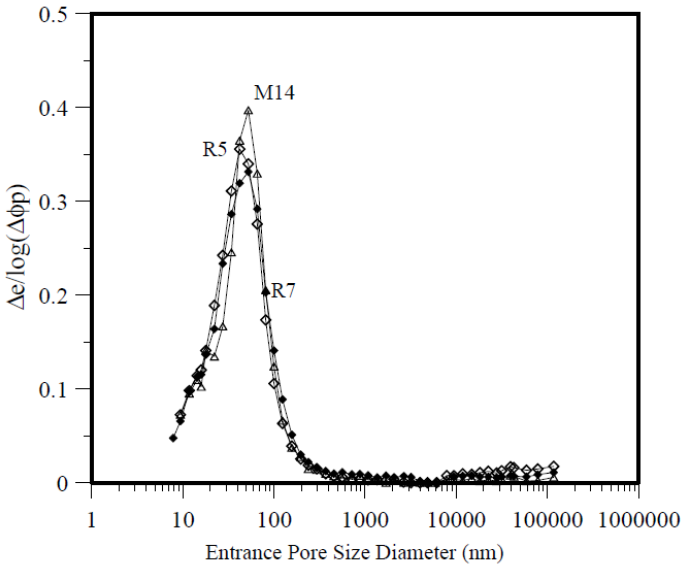

Figure 2.15 PSD curves for dried remolded samples compared with air dried compacted sample (Merchán, 2011)

To gain further insight of the microstructure of drying remolded samples, scanning electron microscope (SEM) photomicrographs done by Merchán (2011) will be analyzed. A sample prepared at a water content 1.3 times the plastic limit (e=1.0, w=0.37) is chosen for analysis because of its similarity to the initial state of samples tested on the adapted ring shear apparatus by Merchán. Figure 2.16 presents the photomicrograph at initial state. Some macroporosity is detected and the presence of some aggregation that was not destroyed during the preparation, however the structure is quite uniform. The after drying photomicrograph is presented in Figure 2.17. The tendency to form aggregation upon drying is evident, however the aggregates seem fused together forming larger and possibly more rigid aggregates. Macroporosity can be observed but as expected the pore size of the macroporosity and microporosity are very similar resulting in the monomodal PSD curve observed in remolded samples.

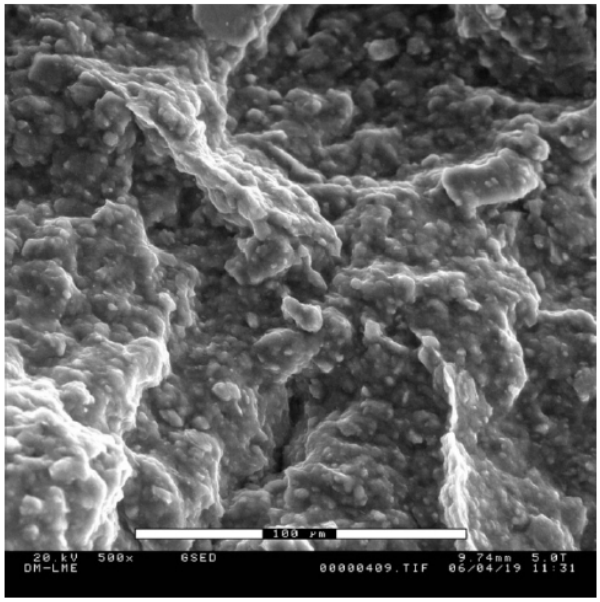

Figure 2.16 SEM photomicrograph for remolded sample at initial state (Merchán, 2011)

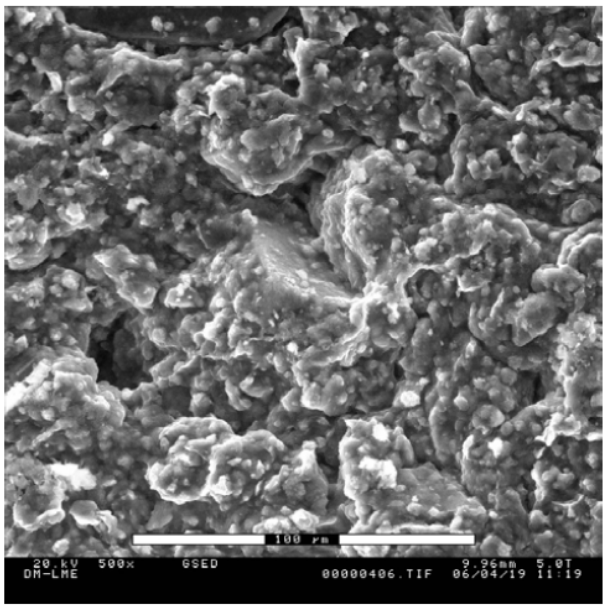

Figure 2.17 SEM photomicrograph for remolded sample after drying (Merchán , 2011)

3. Shear Strength of compacted unsaturated Boom Clay at very large strain

3.1. Previous works on residual shear strength and effective stress of unsaturated clay

As has been stated, the shear strength of soils is fundamental in many geotechnical engineering applications. Traditionally the shear strength of soils for saturated states has been determined using the effective stress proposed by Terzaghi (1936) with the Mohr-Coulomb failure criterion.

$$\tau = c' + (\sigma - u_w)tan\varphi' \quad \text{(eq. 2.4)}$$

Where c' is the apparent cohesion, σ is the net normal stress, u_w is the pore water pressure and φ' is the internal friction angle of the soil. Bishop (1959) introduced an effective stress variable for unsaturated soils that could be used for the determination of shear strength.

$$\sigma' = (\sigma - u_a) - \chi(u_a - u_w) \quad \text{(eq. 2.5)}$$

Where u_a is the pore air pressure and χ is an effective stress parameter which has a value of 1 for saturated soils and a value of 0 for dry soils. The difficulty with this definition of effective stress is the determination of χ. Many attempts have been made to find a relationship between χ and the degree of saturation but it has been observed that the parameter is also related to the structure (Khalili and Khabbaz, 1998).

Fredlund and Morgensten (1977) proposed another equation for the shear strength of unsaturated soils. They defined unsaturated soils as a four phase system composed of two phases that come to equilibrium under applied gradients and two that flow under applied pressure gradients. Three different stress states variables were proposed, (σ-u_w), (u_a-u_w), and (σ-u_a) and any two combination of the three can be used to define the stress state. The failure surface defined with these stress states as follows.

$$\tau = c' + (\sigma - u_a)tan\varphi' + (u_a - u_w)tan\varphi'' \quad \text{(eq. 2.6)}$$

Where φ'' is the friction angle with respect to changes in (u_a-u_w) when the net normal stress is held constant (Fredlund et al., 1978). It has been observed that the value of φ'' is not constant and varies with suction, resulting in a nonlinear failure envelope with respect to suction. The value of φ'' often begins with a value similar to the internal friction angle, and as suction increases it becomes lower until reaching a constant value (Gan and Rahardjo, 1988).

More recent attempts to incorporate the microstructure of soils into and effective stress definition have been made. Alonso et al. (2010) proposed a Bishop like equation for the shear strength of unsaturated soils where the parameter χ is defined as an effective degree of saturation that takes into account water -filling the inter-aggregate pores. They proposed that the effective stress in unsaturated soils cannot be separated from the soil microstructure and for that reason a distinction was made from water filling the macropores and the micropores. Alonso et al. (2013) introduced an additional state variable to take into account the microstructure of compacted soils in the definition of effective stress. The ratio of microvoid ratio to total void ratio is presented ξ_m which has a pattern established throughout the compaction plane.

As has been shown the shear strength of unsaturated soils has been a subject of study for some time, but the residual shear strength has only been researched in the recent year. Sedano et al. (2007) developed and adapted ring shear device that used axis translation technique to apply suction on the soil specimen up to

500 kPa. Vaunat et al. (2006) also presented a modification of the Bromhead ring shear apparatus with a rubber cap with inlets allowing suction imposition through the vapour transfer technique. Tests were done on a low plasticity clay and a slight increase in residual shear strength with high suction was found. Merchán (2011) did a further adaptation of the Bromhead ring shear device and tested remolded samples of Boom Clay at high suction. A significant increase in residual shear strength was observed, particularly an increase in internal friction angle. Velosa (2011) also presented another adaptation of the ring shear device for applying suction through axis translation technique up to a maximum of 500 kPa. Tests were performed in silty sand, silty clayey sand and silty clay. Again an increase in residual shear strength was observed. The results from Velosa (2011) and Merchán (2011) are presented in more detail in section 3.5.1 and used for comparison.

3.2. Ring shear tests

3.2.1. Adapted Bromhead Ring Shear Apparatus

To study the effect of suction in the residual shear strength of clay, an adapted ring shear apparatus was used. The adaptation was developed by Merchán (2011) to be able to apply and control high total suctions in soil. It uses vapour equilibrium technique which allows the application and control of total suctions ranging from 3 to 300 MPa. Figure 3.1 shows the scheme of the circuit used to apply the vapour transfer technique.

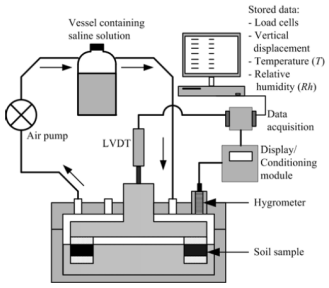

Figure 3.1 Scheme of the experimental setup with ring shear cell, vapour transfer system and data acquisition (Merchán; 2011).

For the investigation a modified version of the apparatus was used. The soil was prepared at a target water content and dry density, therefore the Adapted Bromhead Ring Shear Apparatus was used to isolate the soil and maintain the applied water content. This was achieved through a glass made chamber assembled to the torque arm of the ring shear. Silicone grease was used to tight the interfaces between the glass chamber and the torque arm. For the interface between the glass chamber and the ring shear outer base, lubricating oil was used to reduce the friction between the glass and the base. Figure 3.2 presents the cross section of the chamber mounted on the ring shear device.

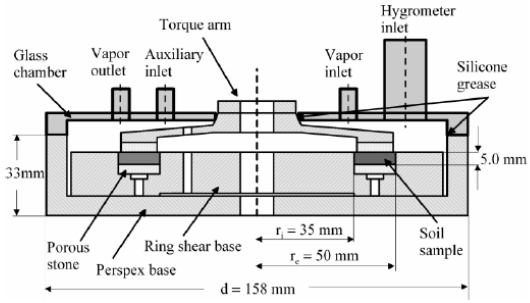

Figure 3.2 Cross section of the glass chamber adapted to the ring shear cell (Merchán; 2011).

The glass chamber consists of four connections, an inlet and an outlet for vapour transfer, an inlet for placement of the hygrometer and one auxiliary inlet. For the testing the auxiliary inlet and the inlet and outlet for vapour transfer were sealed with silicone to achieve isolation of the chamber. Only the hygrometer inlet was used to measure relative humidity and temperature inside the chamber. Relative humidity and temperature readings were taken manually during each loading stage. Measurements of the shear stress through the load cells in the torque arm, and vertical displacement with an LVDT were taken automatically and stored in a computer. Figure 3.3 presents an image of the experimental setup.

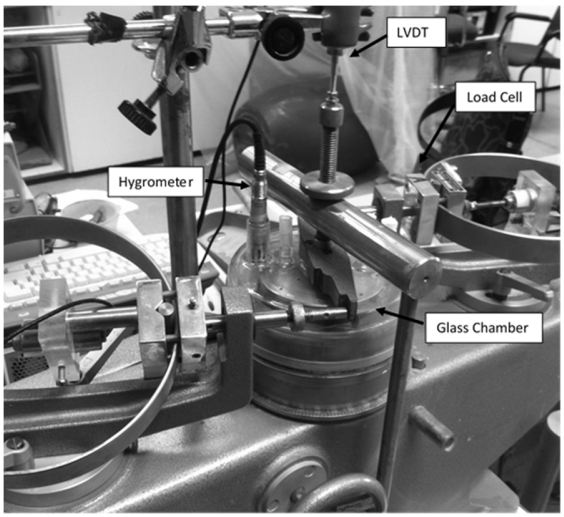

Figure 3.3 General view of the adapted ring shear setup

3.2.2. Sample preparation

The testing program consists of a number of samples prepared at low water contents, and four different void ratios. The soil water content range was selected from hygroscopic water content, approximately w= 3%, to w= 12% which corresponds to saturation of the microstructure S_{rm}= 1 for Boom Clay (Romero; 1999). The water contents selected correspond to a range of matric suction s up to 147 MPa, hence the

effect of suction in the microstructure of the soil can be studied. The procedure followed for the preparation of the specimens is described as follows.

- Blocks of natural Boom Clay were exposed to air during 48h and subsequently crushed with a rubber hammer and passed through a No. 40 (425 μm) ASTM sieve to obtain a clay powder which was left 24h to achieve equilibrium in the laboratory with an average 50% humidity.
- The clay powder was divided into portions to prepare at different target humidity. The amount of added water necessary for each target water content was calculated and the soil was sprayed with a fine mist of demineralized water and thoroughly mixed.
- The soil water mixture was passed through a No. 10 (2mm) ASTM sieve to break down large aggregates due to uneven wetting of the soil. This way maximum clay aggregate size was controlled.
- The soil was placed in metallic bowls sealed with plastic and left in a humidity chamber for at least 24h to achieve a homogeneous water content throughout the samples.
- A mold was designed by Romero (personal communication) to statically compact the soil in the ring shearing base using a mechanical press. The maximum displacement of the mold was limited preventing over compaction of the sample. The mold is compressed to achieve a predetermined dry unit weight $\gamma_{d.}$
- The weight of clay powder necessary to achieve the target $\gamma_{d,}$ was evenly placed in the ring shear base with the mold and compacted in the mechanical press to a preset stress and allowed to stabilize. The stabilization time was short due to the lack of large pore water pressures. This process was repeated twice for each $\gamma_{d,}$-*w* combination. The first sample was used to determine the matric suction *s* using a dewpoint potentiometer (WP4, Decagon Devices). The second sample was sheared using the Modified Bromhead Ring Shear Apparatus.

A total of 17 samples were tested corresponding to different void ratios *e* and water contents *w*. Figure 3.4 and Table 3.1 presents the range of values selected for testing. The range was selected to include loose to dense samples and water contents from hygroscopic water content to water content corresponding to a saturated microstructure. A saturated sample was tested as reference.

Slight variations in water content during the shearing process were observed due to the lack of sealing between the glass chamber and the shearing base. This accounts for slight differences in results corresponding to the last shearing stage, σ_v = 200 kPa, where the drying was more noticeable.

Table 3.1 State conditions for compacted samples.

Sample	*e*	*w*	Sr
S1	0.80	0.036	0.12
S2	0.59	0.036	0.17
S3	0.93	0.037	0.11
S4	0.69	0.038	0.15
S5	0.93	0.039	0.11
S6	0.80	0.042	0.14
S7	0.69	0.045	0.18
S8	0.54	0.056	0.28
S9	0.54	0.07	0.35
S10	0.93	0.073	0.21
S11	0.93	0.08	0.23
S12	0.54	0.085	0.42
S13	0.54	0.11	0.55
S14	0.69	0.118	0.46
S15	0.93	0.112	0.33
S16	0.80	0.129	0.44
S17	0.93	0.345	1.00

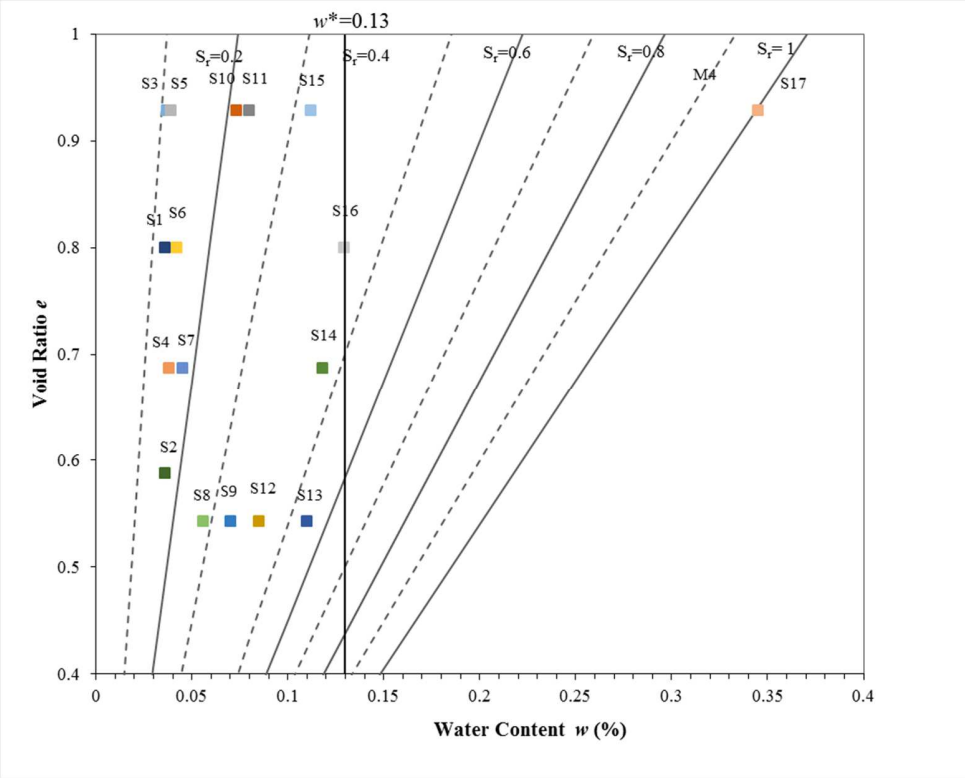

Figure 3.4 Statically compacted samples.

3.2.3. Test protocols

The testing program consists of multi stage shearing tests on each of the samples prepared. After the samples are prepared and compacted as described in section 3.3.2 they are placed in the modified Bromhead Ring Shear device. The glass chamber, which is attached to the torque arm, is lined with lubricating oil to reduce friction during the shearing process. The torque arm and glass chamber are then placed on the shearing device and the system is closed to begin the process. The multi stage shearing is done with net vertical stresses σ_v of 50, 100 and 200 kPa. For each net vertical stress σ_v the sample is allowed a consolidation period of 20 minutes. Since the water contents *w* correspond to dry inter aggregate pores, consolidation time of 20 minutes was observed to be enough for vertical displacement stabilization. After consolidation the shearing stage begins, the shear rate employed was 0.089 mm/min which maintains a stable stress ratio for samples in saturated and dry states (Merchán; 2011). The shear displacements were maintained until a constant value for shear stress was reached which was observed to be a minimum of 100 mm.

Once the shearing stage was complete and the process was repeated for each vertical confining stress, the sample was weighed to determine the weight of material lost during shearing. Final water content for each sample was also measured to determine the change in suction of the sample.

3.3. Experimental results

The testing was done on samples prepared to a specific water content as detailed in section 3.3.2 in order to compare with previous tests done by Merchán (2011) in which total suction was applied on a vertically loaded sample starting from relatively high initial water contents. The main difference between Merchán and the current testing program is the control of clay aggregate size through a sieve (besides starting from relatively low water content), which ensures keeping constant their maximum size in all specimens. The only variable in structure is that caused by the imposed moisture content and dry density. Tests were executed at different void ratios. Experimental results of the multi-stage shearing results are presented in Table 3.2 and shear stress-displacement curves of characterizing tests are presented in Figure 3.5 to 3.8.

As shown in these figures, the unsaturated shear stress displacement curves present a ductile behavior with little or no peak strength. Tests done by Merchán 2011 presented a brittle behavior characterized by dilatancy on the onset of peak strength that suggest a sand like behavior of the clay aggregates in unsaturated conditions. This difference suggests the importance of aggregate size and aggregate fusion, caused by imposition of suction, on the stiffness and friction characteristics of unsaturated clayey soils.

The testing displays a slight variation in residual internal friction angle φ_{res} of the soil with the water content. The internal friction angle is taken as the slope of the shear stress (τ) vs. net normal stress (σ_v) curve for each sample. At hygroscopic water contents $\varphi_{res} = 14^o$-16^o while at slightly higher water contents $\varphi_{res} = 10^o$-

12°. Figure 3.9 presents the relationship between residual shear stress and water content for different void ratios, it is observed that void ratio appears to have no significant effect on the residual shear strength of the soil. Other authors have observed the lack of influence of initial dry density on the residual shear strength of unsaturated soils.

Table 3.2 Ring shear multistage test results.

Sample	*e*	*w*	Sr	Ψ(MPa)	σ_v (kPa)	τ_r (kPa)	φ_{res}
S1	0.80	0.036	0.12	147	50	16.1	14.1
					100	23.4	
					200	50	
S2	0.59	0.036	0.17	147	50	14.2	14.8
					100	28	
					200	51.7	
S3	0.93	0.037	0.11	140	50	16.2	16.6
					100	31.9	
					200	58.1	
S4	0.69	0.038	0.15	134	50	16.4	14.2
					100	25.1	
					200	50	
S5	0.93	0.039	0.11	129	50	17.1	15.7
					100	27.8	
					200	55.7	
S6	0.80	0.042	0.14	103	50	15.2	13.5
					100	25.7	
					200	51	
S7	0.69	0.045	0.18	71	50	15	14.1
					100	26.1	
					200	48.4	
S8	0.54	0.056	0.28	65	50	12.8	12.6
					100	22.4	
					200	44.4	
S9	0.54	0.07	0.35	37	50	11.4	11.8
					100	21.5	
					200	41.1	
S10	0.93	0.073	0.21	33	50	11.5	11
					100	20.1	
					200	38.1	
S11	0.93	0.08	0.23	26	50	10.1	11.5
					100	18.2	
					200	42	
S12	0.54	0.085	0.42	25	50	10.7	11.8
					100	21	
					200	41.5	
S13	0.54	0.11	0.55	22	50	10.5	11.3
					100	19.6	
					200	-	
S14	0.69	0.118	0.46	13	50	11.1	9.7
					100	18.3	
					200	33.1	
S15	0.93	0.112	0.33	20	50	11.1	10.8
					100	18.6	
					200	38.1	
S16	0.80	0.129	0.44	8	50	11	10.1
					100	17.5	
					200	35.2	
S17	0.93	0.345	1.00	0	50	9.7	11
					100	19	
					200	-	

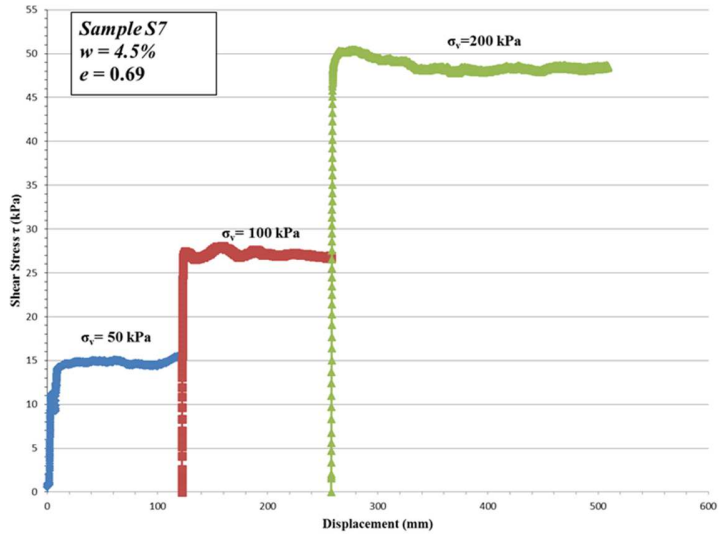

Figure 3.5 Shear stress-displacement curve for sample S7.

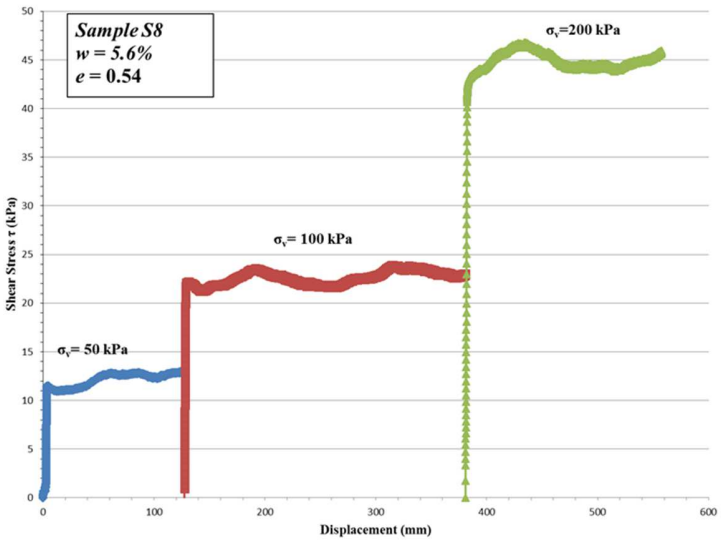

Figure 3.6 Shear stress displacement curve for sample S8.

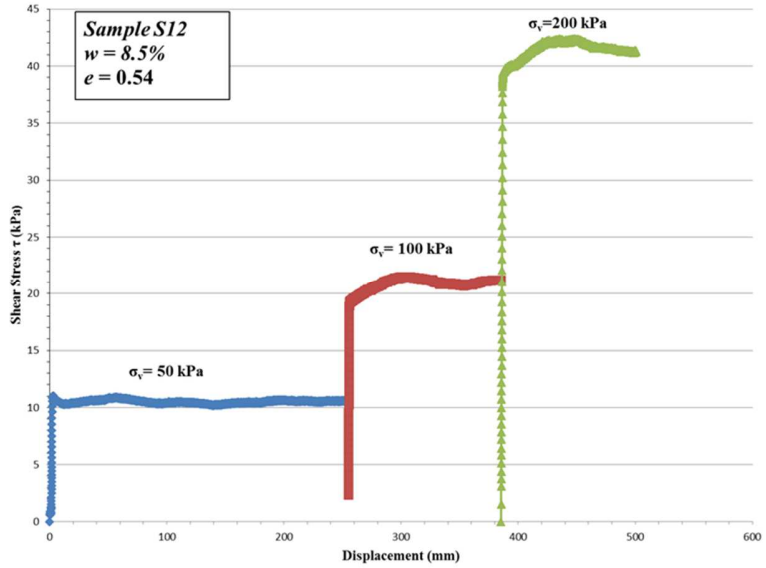

Figure 3.7 Shear stress displacement curve for sample S12.

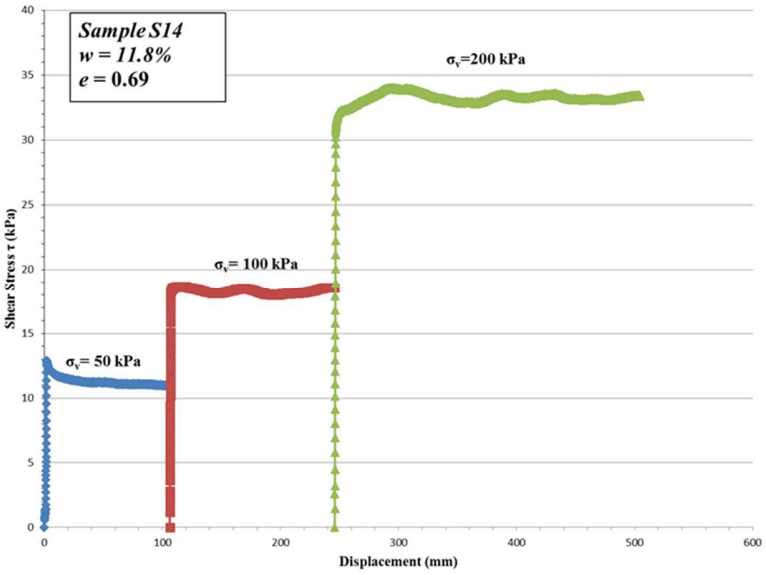

Figure 3.8 Shear stress-displacement curve for sample S14.

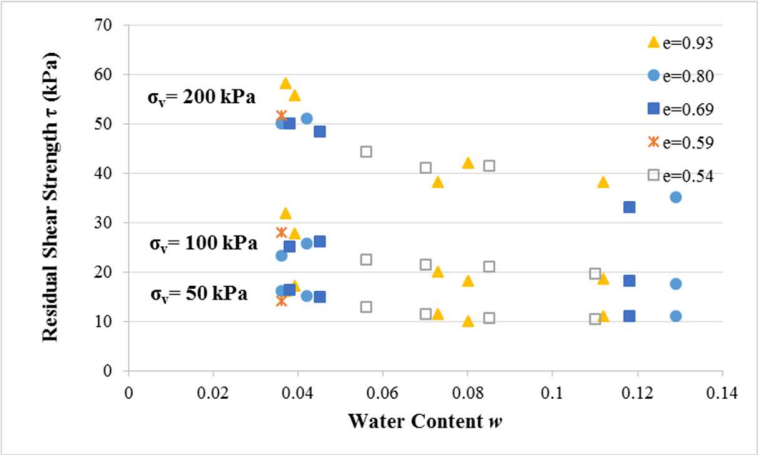

Figure 3.9 Residual shear strength as a function of water content for all samples with different void ratios.

Samples tested at low water contents were in a powder state which presented material loss during the shearing process. This accounts for the increased "noise" observed in the shear strength curves. The difference between the highest or lowest value of stress and the average residual value of stress is about 3.5 kPa which in some cases represented a difference of 10%. As water content *w* increased the material loss decreased and the "noise" was reduced to a maximum difference of 5% in some samples. For the analysis the average value was considered. The material lost in all samples accounts for the lack of stabilization of the vertical strain as would be expected when residual state has been achieved.

The residual failure envelopes are presented in Figure 3.10 for all samples tested. The failure envelopes present R squared values ranging from 0.9637 to 0.9997 with a y intercept equal to 0 as is expected for residual failure envelopes. It is important to note that no cohesion is observed in any of the samples tested even though traditionally an increase in suction has been associated with an increase in cohesion in shear strength. The highest residual angles correspond to the highest matric suctions, as suction decreases, φ_{res} slightly decreases until it reaches the saturated residual strength when *w*= 7.3%. It was observed that when Sr_m reaches a value of approximately 0.50, the residual strength of the unsaturated Boom Clay reaches the saturated residual strength of Boom Clay which in this study was determined to be $\varphi_{res}= 11^o$. Previous works have found the saturated residual friction angle of Boom Clay to be slightly higher, ranging from 13^o to 18.5^o (Bouazza et al., 1996; Coll, 2005; Merchán, 2011; Deng et al., 2011).

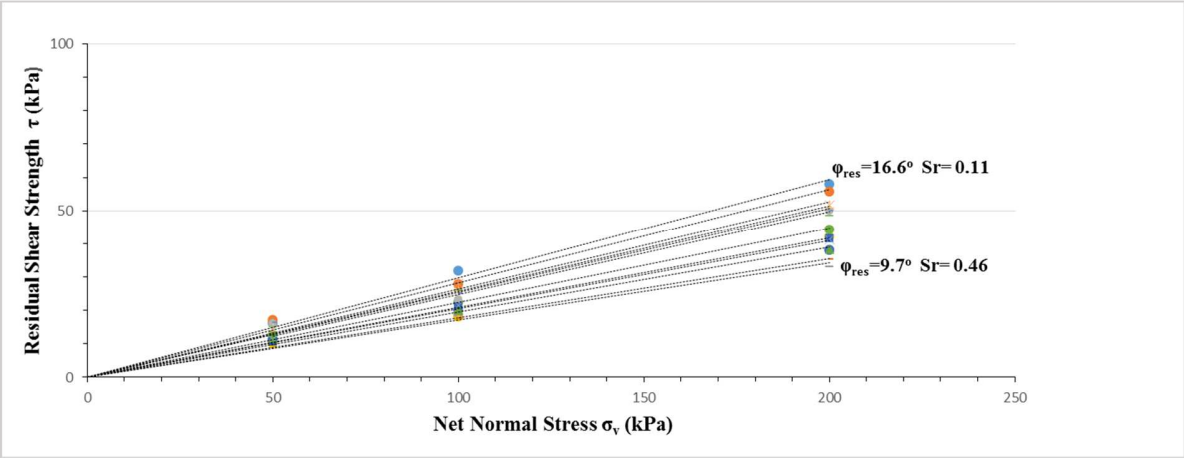

Figure 3.10 Residual strength envelope for Boom Clay samples with different degree of saturation.

3.4. Interpretation of experimental results

In this section an interpretation of the experimental results will be presented and for that purpose a micro structural viewpoint will be explored. For a first analysis the normalized residual strength is used in order to more clearly determine trends in the residual shear strength with different variables. The normalized residual strength is defined as the ratio of shear stress to normal stress (τ/σ_v). Figure 3.11 presents the normalized residual stress with respect to the normal stress. As has been observed before, residual strength decreases with the decrease in suction, but also a slight decrease in normalized residual strength with the increase of normal stress can be noticed. This suggests a minor nonlinearity of the residual shear strength failure envelope for Boom Clay. Nonlinear failure envelopes for clayey soils have been observed by several authors in previous works (Stark & Eid, 1994; Lupini et al., 1981; Fredlund et al., 1987). The nonlinearity is determined to be minor and thus for the purpose of analysis a linear failure envelope has been used to determine the value of the internal friction angle φ_{res},

As shown in the previous section, an increase in shear strength with suction is evident, but the relationship between the shear strength and suction is not as evident. Figure 3.12 shows the relationship between the residual internal friction angle and total suction for all samples tested. The increase in residual shear strength is not linear, it presents a smooth curvature which suggests a stabilization of the residual shear strength at very high suctions. An additional trend can be observed when the normalized residual strength is graphed as a function of total suction as shown in Figure 3.13. It is observed that at lower suctions the residual strength remains stable and increases gradually with suction until reaching a stable value at high suctions.

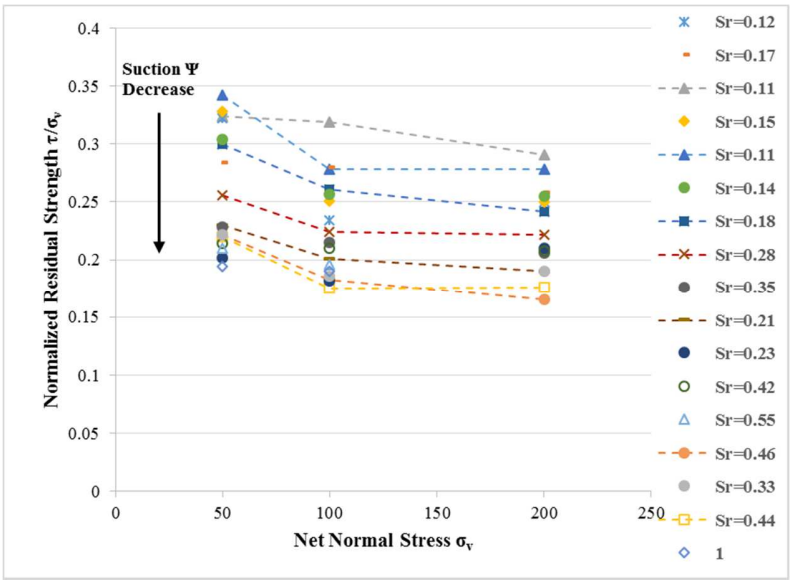

Figure 3.11 Residual stress ratio as a function of net normal stress

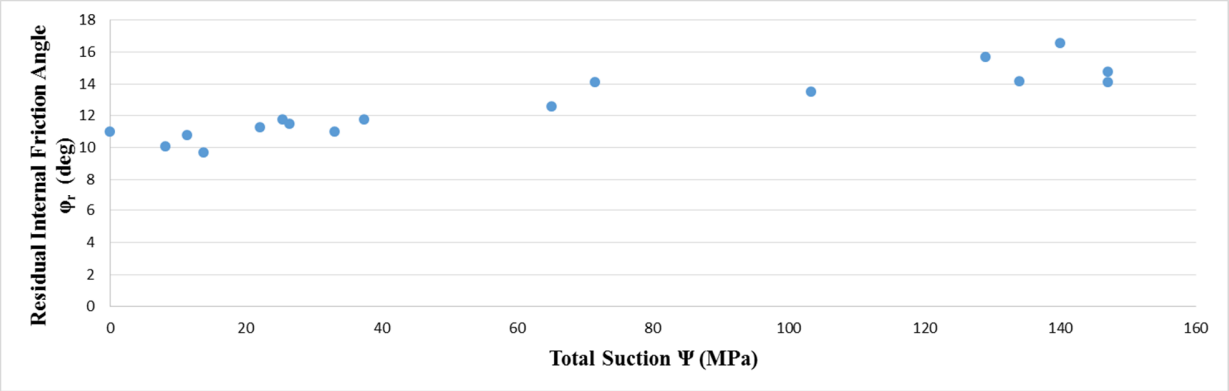

Figure 3.12 Residual internal friction angle as a function of total suction.

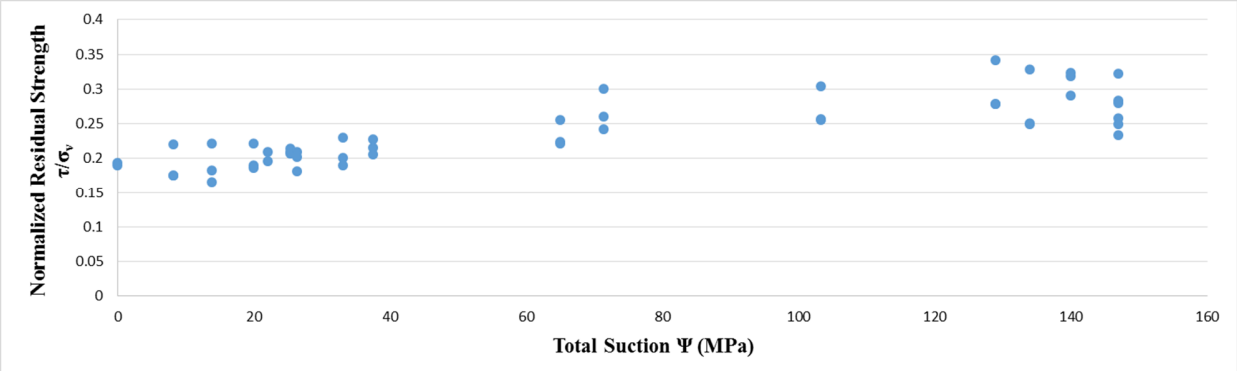

Figure 3.13 Residual strength ratio as a function of total suction.

To further investigate the relationship between residual strength and suction of the soil in unsaturated conditions, the residual strength ratio is presented as a function of the degree of saturation as depicted in Figure 3.14. A decrease in shear strength with an increase of the degree of saturation is evident but a relationship with the microstructure is needed. As presented in section 2, clay aggregates are formed when water is added to clayey soils giving way to a distinct structure consisting of the microstructure and macrostructure. A delimiting value of water content separates both structures, for Boom Clay the value corresponds to w^*= 13% (Romero, 1999). At very high suctions, which is the case, the microstructure becomes desaturated creating a need for a degree of saturation of the microstructure. The degree of saturation Sr for a saturated microstructure S^*_{rm} and degree of saturation of the microstructure can be defined as:

$$S^*_{rm} = \frac{G_s * w^*}{e} \quad \text{(Eq. 3.1)}$$

$$S_{rm} = \frac{S_r}{S^*_{rm}} \quad \text{(Eq. 3.2)}$$

Figure 3.15 presents the normalized residual strength as a function of the microstructural degree of saturation S_{rm}. When the microstructure is saturated, the residual strength of the soil is already that of a saturated soil. For this reason the microstructural degree of saturation seems a more adequate variable for the determination of an effective stress for unsaturated soils than the traditional degree of saturation.

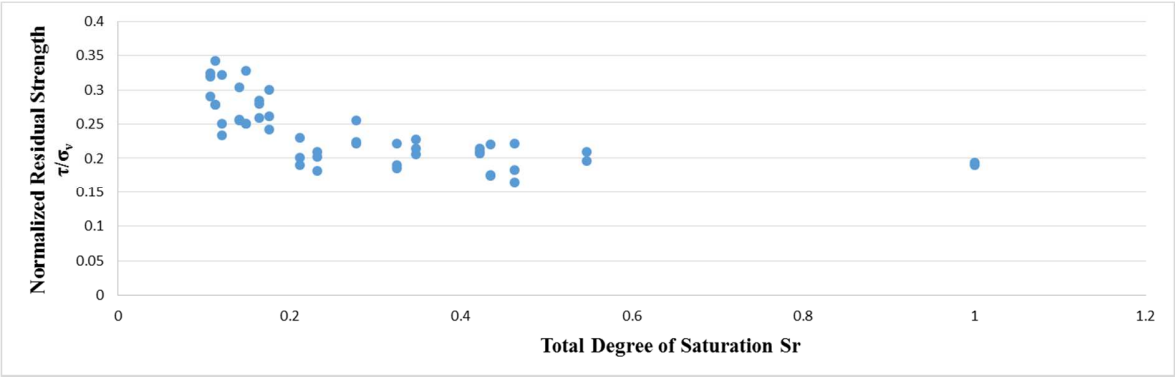

Figure 3.14 Residual strength ratio as a function of the degree of saturation.

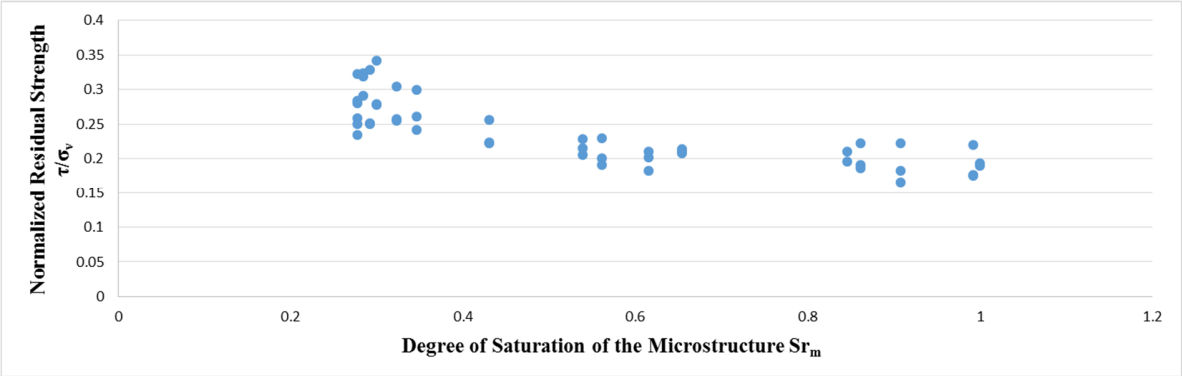

Figure 3.15 Residual strength ratio as a function of the degree of saturation of the microstructure.

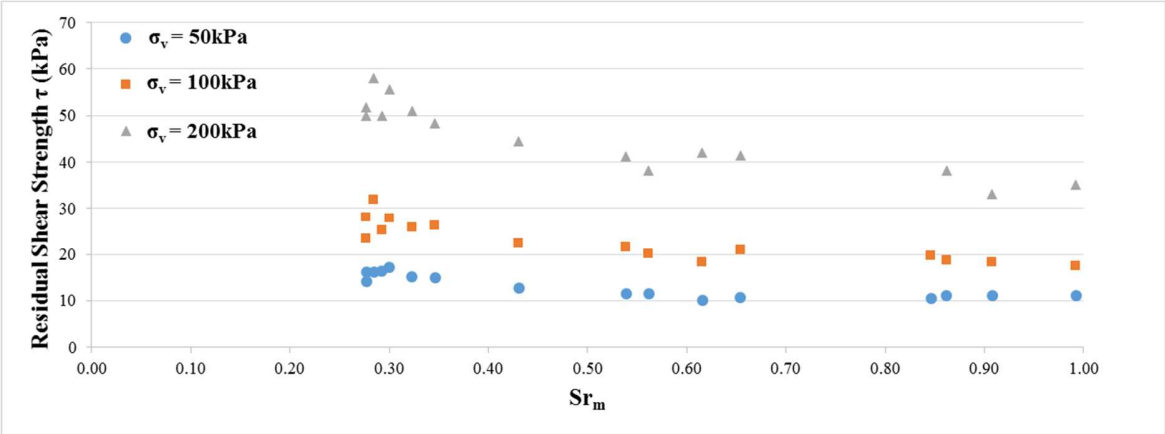

Figure 3.16 Residual shear strength as a function of the degree of saturation of the microstructure for different net normal stresses.

3.4.1. Comparison with previous tests

Previous works have been done on the residual strength of soil at high suction values. More noticeably are the works of Merchán (2011) and Velosa (2011). Both of them used modified ring shearing apparatuses. Velosa developed a Fully Servo/Suction-Controlled Ring Shear that consisted of a fully servo-controlled system similar to that of the original ring shear apparatus developed by Bromhead (1979). In it tests could be performed either on remolded or statically compacted test specimens. Merchán used the Adapted Bromhead Ring Shear Apparatus developed by Vaunat et al (2006) which is the same used in this work.

Velosa (2011) performed tests on three different soils, silty sand (SM), silty clayey sand (SM-SC), and silty clay (CL) and performed single and multi-stage tests on a low matric suction range from 0 to 100 kPa. Some samples were prepared at target water contents corresponding to the desired suction, the rest were prepared at water contents 6% greater than proctor optimum and later soaked with distilled water inside the chamber. In all cases the samples were compacted to a desired density and while inside the chamber loaded with a net normal stress of 25kPa and allowed to consolidate for 24 h. Afterwards the equalization stage begins in which water content is adjusted to achieve the target suction. The test results are summarized in Figure 3.17. An increase in residual friction angle with suction can be observed for the SM and SM-SC soils but also an increase in cohesion. In addition the samples presented peak behavior with dilatancy that increased with suction, but it was only observed during single stage tests and the first shearing of multi-stage tests. The increase in cohesion observed in these tests is not contradictory with the results of this study where no increase in cohesion was observed. The range of suction tested is much lower, in levels where the microstructure is saturated and there is inter-aggregate water causing a capillary effect because of the menisci formed in the macropores that can result in an increase in cohesion. The results were inconclusive for the CL soil because it appeared that the increase in residual shear stress increase beyond the maximum

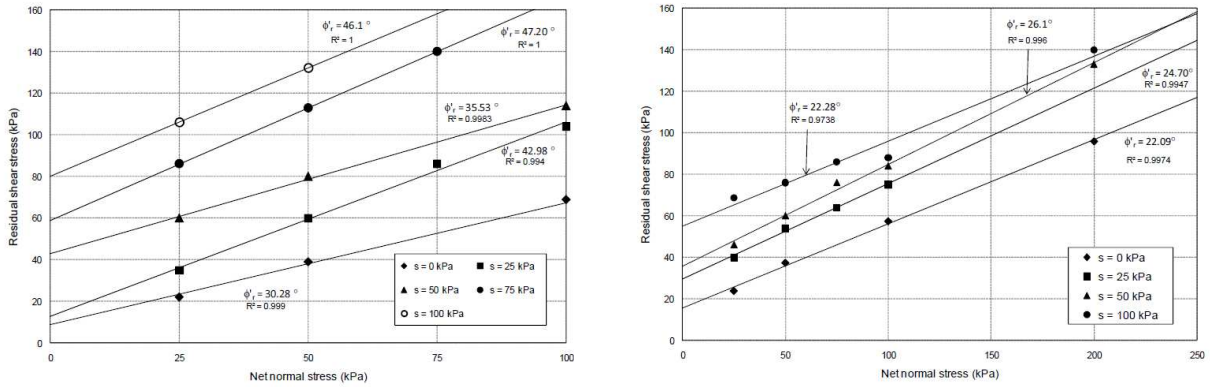

Figure 3.17 Effect of matric suction state on residual failure envelopes for (a) compacted SM soil and (b) compacted SC-SM soil (Velosa, 2011).

capacity of the sensors.

Merchán (2011) performed tests on Boom Clay using the same apparatus used on this work, therefore the results will be used for direct comparison with the results obtained in this work. The main difference between the tests performed by Merchán is the preparation of the sample, and the application of suction. For the tests performed by Merchán the specimens were prepared at a water content above the plastic limit and below the liquid limit of the soil. Most tests done had initial water content of w_0=34% and w_0=40% while a few were done with w_0=5.4%. In all cases soil suction was achieved through vapour transfer technique by placing the sample in the adapted Bromhead Ring Shear Apparatus and closing the system

with a relative humidity corresponding to the suction targeted. The sample was first loaded with a vertical net stress ranging from 25 kPa to 300 kPa and after consolidation, total suction was applied by connecting the air pump and allowing equilibrium. The difference in sample preparation leads to a great difference in microstructure despite samples being in the same state.

The test results differ from the ones obtained in this study. First, Merchán observed a very large increase in residual shear strength with suction. Figure 3.18 presents the variation in residual internal friction angle for some of the samples tested. The increase was consistent in all samples with various initial water contents. In this study the increase in residual shear strength with suction was significantly lower as was presented in section 3.4. Although both investigations coincide in the absence of cohesion in unsaturated clays at residual strengths. A comparison of the results obtained in both investigations is presented in Figure 3.19. The slope of the curve created by Merchán's results is much steeper than the results from this work for all net vertical stresses. Likewise the saturated residual strength is slightly higher in the results by Merchán.

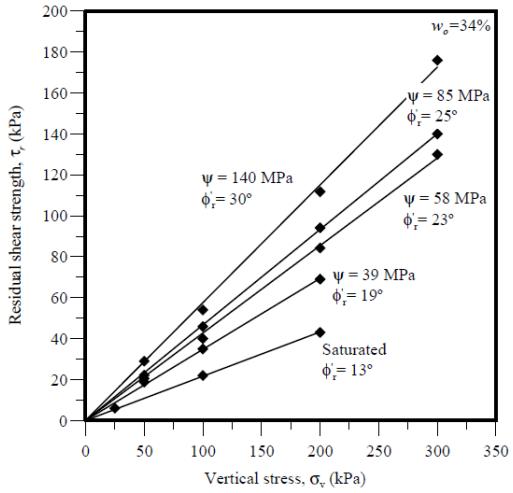

Figure 3.18 Envelopes of residual strength on Boom Clay samples at different target total suctions (Merchán, 2011).

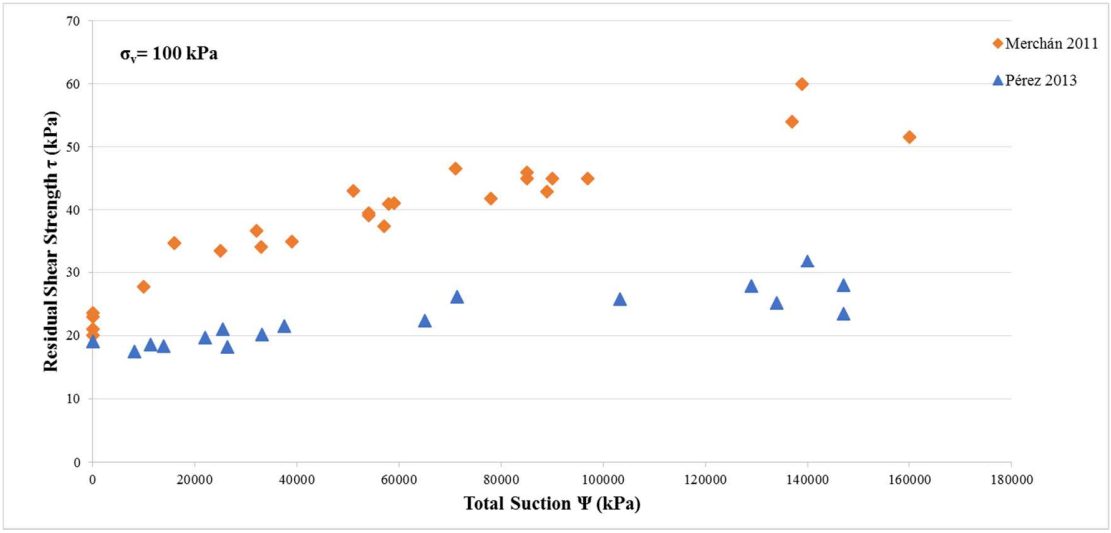

(a)

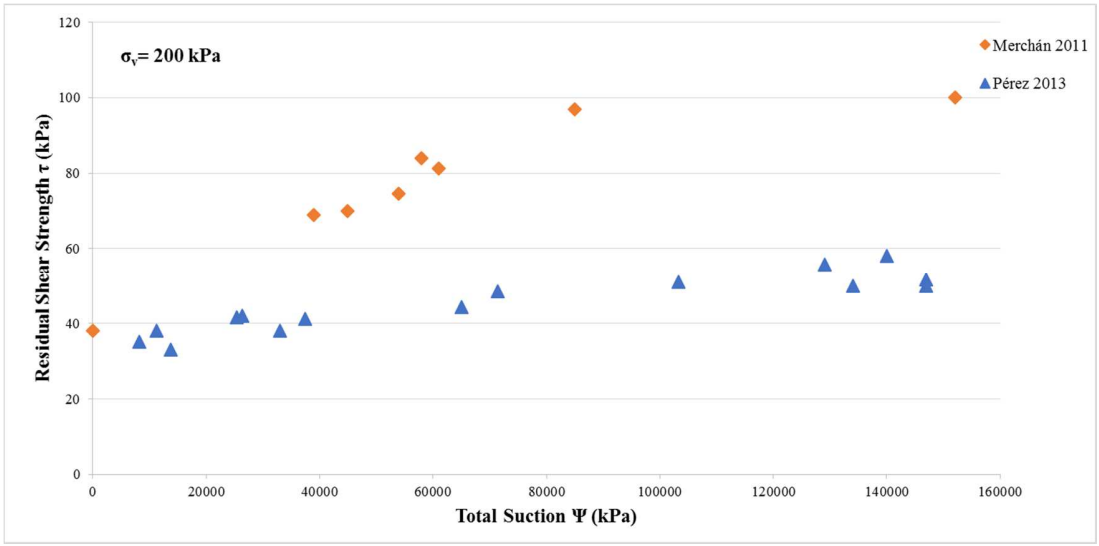

(b)

Figure 3.19 Comparison of residual shear strength as a function of total suction of experimental results for net vertical stresses of (a) 100 kPa and (b) 200 kPa.

The second difference is that Merchán's shearing curves were characterized by peak strengths during the first shearing stage that increased with suction. The peak strength was accompanied by a dilatant behavior that resembles the behavior of frictional materials. Furthermore residual strength was reached sooner in unsaturated states than saturated states which suggests an important loss of interlocking of the rigid clay aggregates once dilatancy is fully developed on unsaturated samples. The peak values observed for samples

prepared at higher water contents were noticeably higher than those prepared at lower water contents as can be observed in Figure 3.20. On tests performed during this study no evidence of dilatant behavior was found for any suction value instead a ductile behavior with little or no peak strength characteristics was observed. It seems the drying process stiffens the soil causing dilatant behavior, was a soil prepared and compacted at a specific suction does not present significant stiffness increase and therefore no peak strength and dilatant behavior.

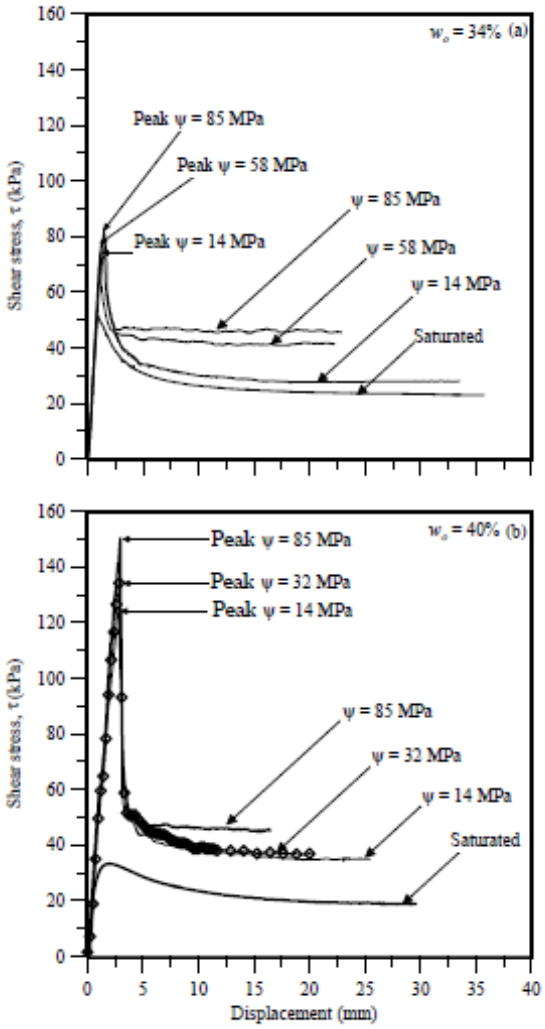

Figure 3.20 Shear stress-displacement curves at different target suctions for initially remolded saturated samples prepared at: (a) w_o= 34% and (b) w_o= 40% (Merchán 2011).

Previous studies have concluded that material history has no influence on the shear strength characteristics of soils (Merchán, 2011; Skempton, 1965; Tarantino, 2005; Velosa, 2001). But the differences between the results obtained by Merchán and the results obtained in this study on the same material point to a strong

influence of sample preparation on soil microstructure and therefore an influence of initial water content and suction history of the material. The double structure of clay as a result of aggregates formed when water is added has a strong influence on the residual shear behavior. In this study the size of aggregates was controlled by preparing the sample at the desired water content to obtain a specific suction and then passed through a No. 10 (2mm) ASTM sieve. The aggregates formed in the tests by Merchán were not controlled in any way and were influenced by the initial water content and the suction applied. Larger interlocked aggregates could be created that contributed to the large increase in residual shear stress of the material. In both previous works on the residual shear strength of unsaturated soils using ring shear apparatuses the initial water content and suction of the material was modified after the application of a confining stress and therefore such an increase in residual shear stress was observed.

3.4.2. Effective stress for compacted clay

In this section an effective stress for compacted soils will be defined from a micro structural viewpoint. In section 3.5 different variables were explored to determine which were appropriate to describe the residual shear strength behavior of compacted clay. It was determined that the degree of saturation plays an important role in defining the effective stress of unsaturated soils. Several definitions for effective stress were explored, Alonso et al. (2010) proposes an effective stress that uses and effective degree of saturation S_e and suction defined as follows.

$$\sigma_v'' = \sigma_v' + S_e * s \quad \text{(Eq. 3.3)}$$

$$S_e = \langle \frac{S_r - S_{rm}^*}{1 - S_{rm}^*} \rangle \quad \text{(Eq. 3.4)}$$

Where *s* is the matric suction and S^*_{rm} is the degree of saturation of the saturated microporosity which for Boom Clay has a value ranging from 0.38-0.65. The value of S_e is equal to zero when the $S_r \leq S^*_{rm}$ and takes values from 0 to 1 when $S_r > S^*_{rm}$. With this definition it is assumed that only water in the macroporosity affects the shear strength of unsaturated soils as has been assumed some studies (Alonso et al., 2010; Alonso et al., 2013). This assumption seems inadequate for the findings of this study as presented in Figure 3.21 where most samples fall within the $S_e = 0$ range. It is observed that when the microstructure is saturated, Boom Clay has saturated residual shear strength; therefore water within the aggregates controls the shear strength of unsaturated soils. Another definition of effective degree of saturation proposed by Romero et al. (1999) for the relative permeability is explored for application.

$$S_e = \frac{w - w_{res}}{w_{sat} - w_{res}} \quad \text{(Eq. 3.5)}$$

Where w_{res} is the residual gravimetric water content and w_{sat} is the saturated gravimetric water content. For the purpose of this study w_{sat} was used as the saturated gravimetric water content of the microstructure. This definition seems more appropriate as it takes into account the water content in the microstructure. However at very high suctions, when the water content approaches the residual water content, the effect of suction on the shear strength equation becomes zero. For this reason a different approach will be used to define an effective stress.

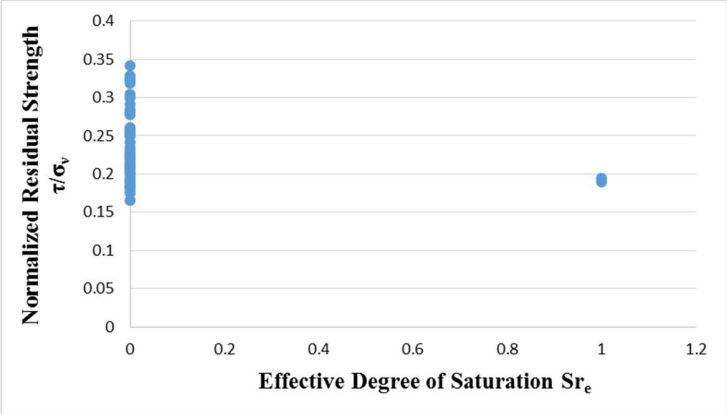

Figure 3.21 Residual stress ratio as a function of the effective degree of saturation.

A similar definition for the effective stress as presented in equation 3.3 is explored using the saturated degree of saturation for the microstructure from equation 3.2.

$$\sigma_v'' = \sigma_v' + S_{rm} * \psi \qquad \text{(Eq. 3.6)}$$

Figure 3.22 presents the normalized residual strength as a function of the new effective stress. It appears adequate as a definition of effective stress, but the influence of suction in this definition is not realistic. Net normal stress has been determined to have more influence on the residual shear strength of unsaturated soils than suction.

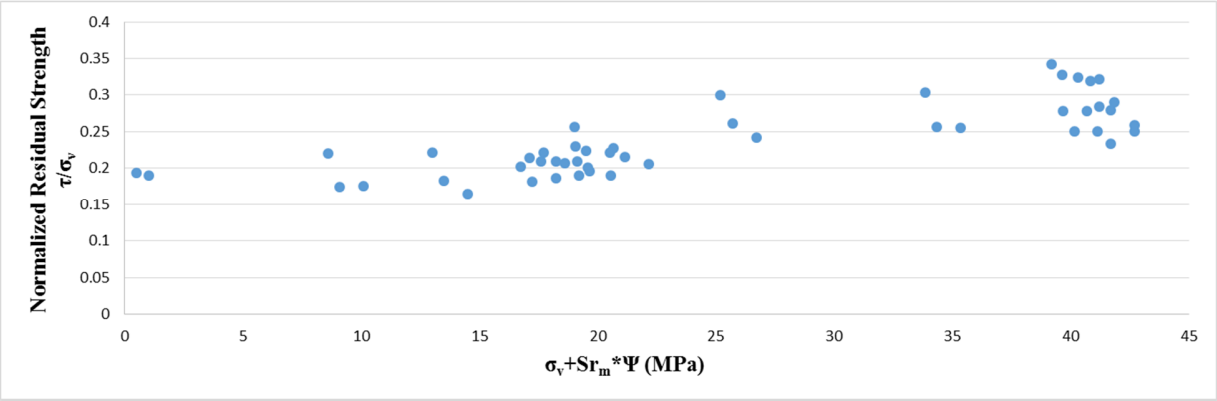

Figure 3.22 Residual stress ratio as a function of the effective stress defined in equation 3.5.

An effective stress that separates the contribution to shear strength of the micro and macrostructure is proposed. It is observed that net stress, degree of saturation and suction appear to control the residual strength at the micro structure. Equation 3.5 presented an effective stress for the microstructure that seemed appropriate to describe the behavior of the Boom Clay at the aggregate level. On the other hand the effective stress of the macrostructure σ'_M is only controlled by the net stress and therefore will be the same as the effective stress in saturated soils σ'_v which for shear strength is the net normal stress σ_v. The proposed effective stress is presented below.

$$\sigma''_v = \sigma'_M + \sigma'_m \quad \text{(Eq. 3.7)}$$

$$\sigma'_M = (1 - a)\sigma'_v \quad \text{(Eq. 3.8)}$$

$$\sigma'_m = a(\sigma'_v + S_{rm} * \psi) \quad \text{(Eq. 3.9)}$$

$$\tau_{res} = (\sigma'_M + \sigma'_m)tan\varphi_{r\,sat} \quad \text{(Eq. 3.10)}$$

It is observed from experimental data that the microstructure does not have the same influence on the effective stress as the macrostructure. A shear strength parameter α is introduced to define the stress distribution between the microstructure and the macrostructure. This parameter is dependent on sample preparation and accounts for the difference in the increase in shear strength observed in Merchán's results from the results of this study. Also it was found that α varies with the net normal stress applied on the sample. To determine the value of α for the different sets of samples least squares regression analysis was performed, Figure 3.23 presents the values of α with respect to net normal stress.

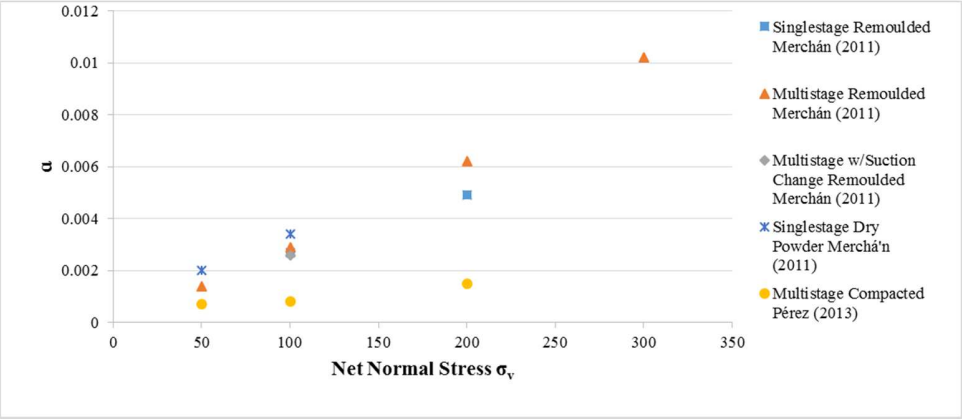

Figure 3.23 Variation of shear stress parameter a with net normal stress for different set of samples tested.

The shear strength parameter α increases linearly with net normal stress, the slope depends on the influence of the vertical stress during the drying of the aggregates and the size of aggregates formed indicating the influence of stress history during the drying process of the sample. When samples are subjected to vertical stress during the imposition of suction, the way it was done in Merchán's tests, aggregates fuse together creating a more rigid structure. This accounts for the significant increase in shear strength observed in Merchán's study and the brittle shear behavior characterized by peak strength. The parameter α is much lower because the aggregate size was controlled, and the slope is also low because there was little or no fusion. In all cases the higher the vertical stress, the higher the influence of suction on shear strength. Figure 3.24 presents the residual strength envelope using the effective stress proposed.

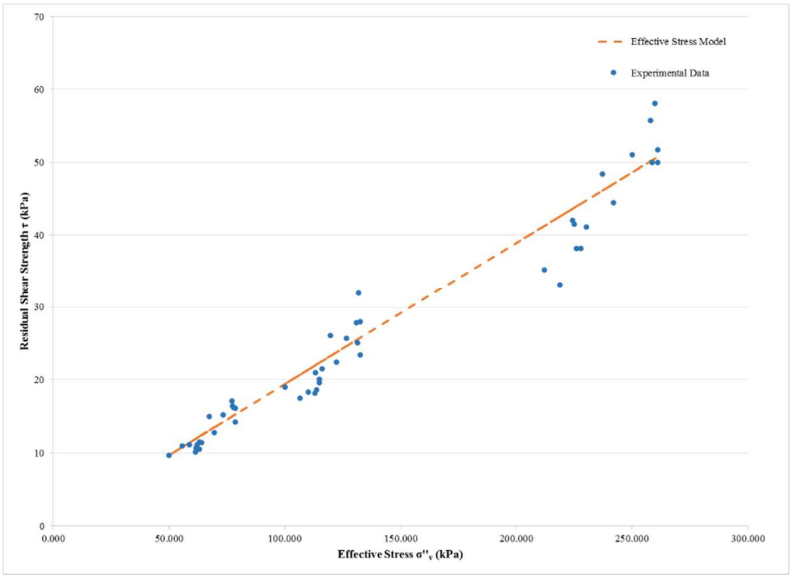

Figure 3.24 Residual strength envelope with the proposed effective stress

Figure 3.24 shows a good agreement between the experimental results and the proposed model for unsaturated shear strength behavior. The slope of the strength envelope is the tangent of the residual saturated internal friction angle as is proposed in the model. This model allows the determination of unsaturated strength parameter from the saturated parameters of the soil.

$$tan\varphi_{r\,sat} = \frac{\tau_{res}}{\sigma_v''} \quad \text{(Eq. 3.10)}$$

$$tan\varphi_r = \frac{\tau_{res}}{\sigma_v'} \quad \text{(Eq. 3.11)}$$

Figure 3.25 shows the variation of residual shear strength with suction for the samples tested compared with the prediction of the proposed model. Again there is good agreement between the predicted shear strength and the experimental data. Samples sheared with a net vertical stress of 200 kPa present a greater scatter compared to samples sheared a lower net stresses. As mentioned in previous sections, this scatter is due to the uncontrolled drying of the samples during the last stages of shearing. Figure 3.26 shows that a normalization of the shear strength can be obtained with the proposed effective stress,

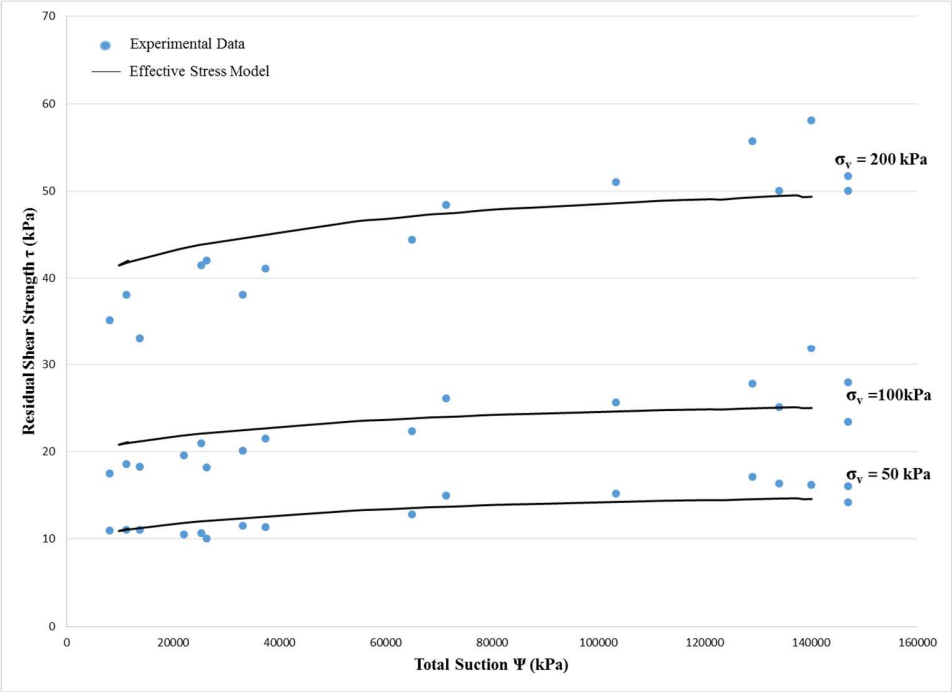

Figure 3.25 Comparison between experimental results and the effective stress model for residual shear stress as a function of total suction.

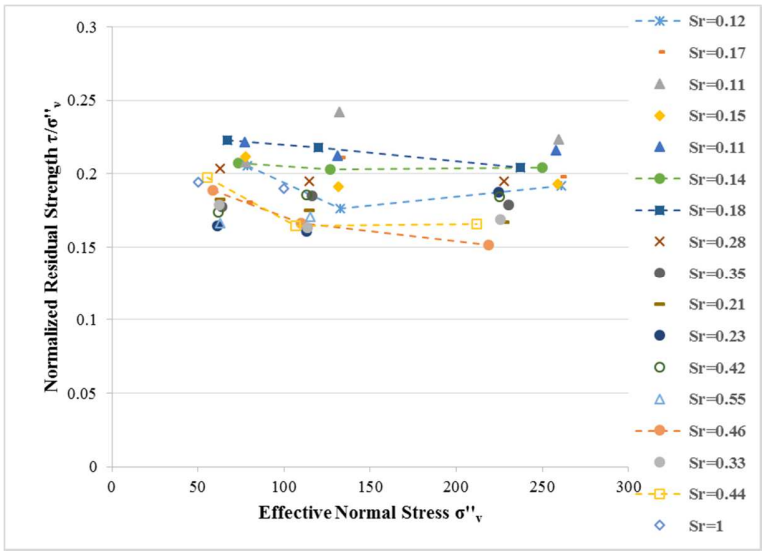

Figure 3.26 Residual stress ratio as a function of effective normal stress.

To verify the validity of the proposed effective stress model in predicting the residual shear strength of unsaturated soils, the model was used to analyze the results reported by Merchán (2011). Figure 3.27 to Figure 3.30 show the residual shear strength as a function of total suction for each of the sets of tests performed with values of α presented in Figure 3.23. The effective stress model is also plotted in each graph, and again the predicted results are in good agreement with the experimental results. Table 3.3 presents the values for the parameter α used for each test set. Figure 3.31 plots the experimental residual shear strength and the predicted residual shear strength for all tests done in this work and by Merchán (2011). The proposed effective stress model proves to be an effective tool for predicting the residual shear stress behavior of unsaturated Boom Clay.

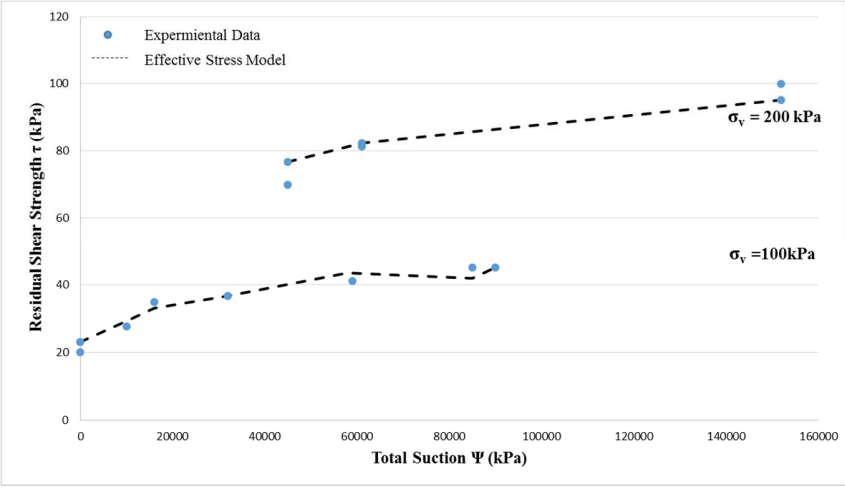

Figure 3.27 Experimental results and effective stress model for residual shear stress as a function of total suction for singlestage remolded tests by Merchán (2011).

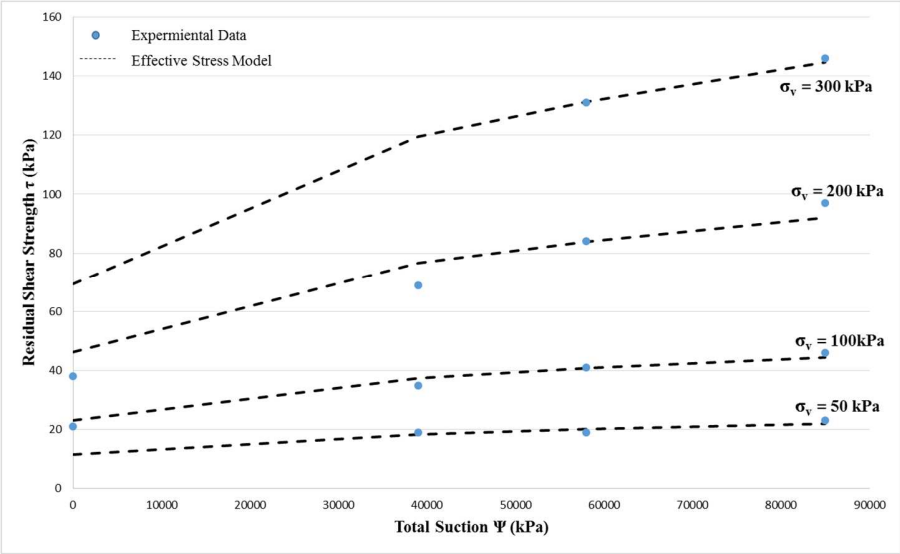

Figure 3.28 Experimental results and effective stress model for residual shear stress as a function of total suction for multistage remolded tests by Merchán (2011).

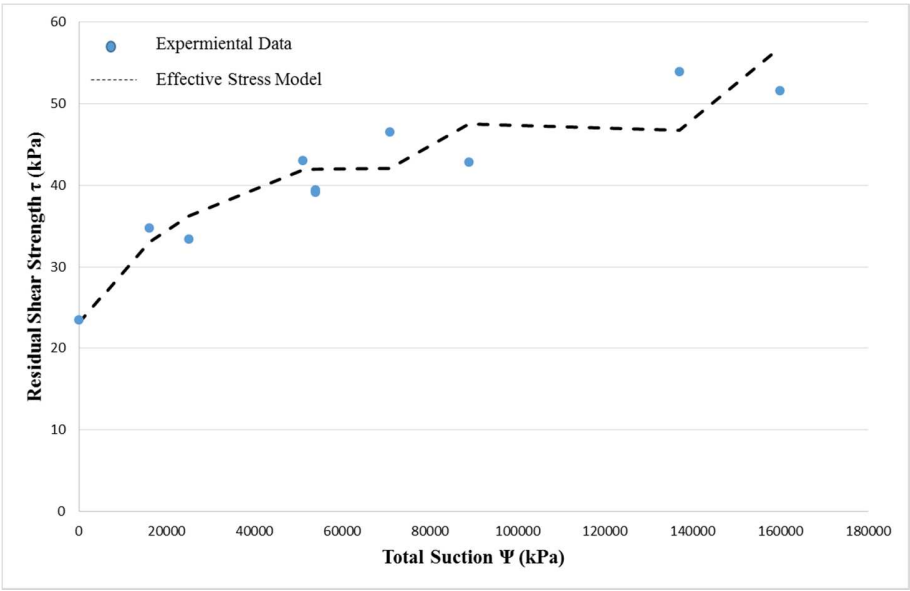

Figure 3.29 Experimental results and effective stress model for residual shear stress as a function of total suction for multistage w/suction change remolded tests by Merchán (2011).

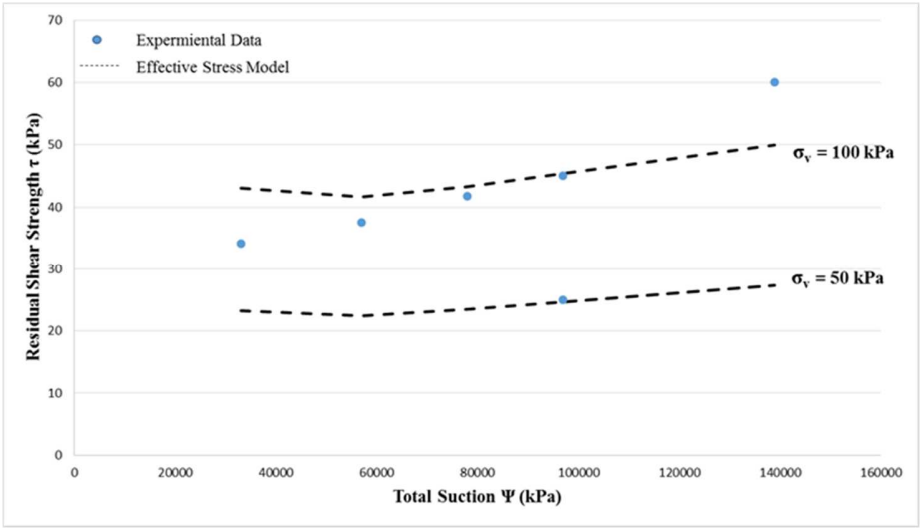

Figure 3.30 Experimental results and effective stress model for residual shear stress as a function of total suction singlestage dry powder tests by Merchán (2011).

Table 3.3 Shear parameter a for different tests.

	Parameter α			
Tests	50 kPa	100 kPa	200 kPa	300 kPa
Multistage Compacted, Pérez (2013)	0.0007	0.0008	0.0015	-
Multistage Remolded, Merchán (2011)	0.0014	0.0029	0.0062	0.0102
Singlestage Remolded, Merchán (2011)	-	0.0027	0.0049	-
Multistage w/Suction Change Remolded, Mechán (2011)	-	0.0026	-	-
Singlestage Dry Powder, Merchán (2011)	0.002	0.0034	-	-

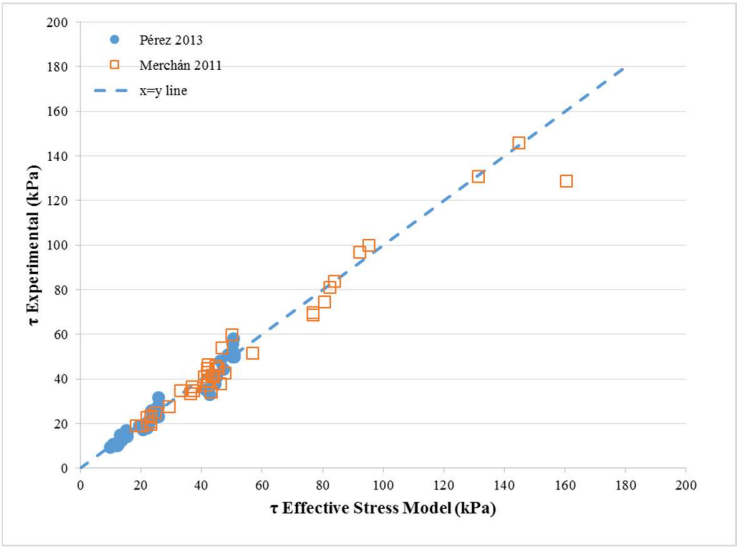

Figure 3.31 Comparison of residual shear strength for experimental values and predicted values using effective stress model.

4. Summary, Conclusions and Future Works

In this study the residual shear strength behavior of unsaturated Boom Clay has been studied from a microstructural viewpoint. The study has been focused on statically compacted samples to simulate the in situ state of compacted clay. To study the microstructural aspects of compacted soils, an in depth literature review has been conducted on the microstructure of compacted and remolded clays. Mercury intrusion porosimetry tests were carried out on selected samples of compacted Boom Clay and the results were compared with previous MIPS tests conducted by Romero (1999) and Merchán (2011). The shear strength of compacted Boom Clay at very large strain was studied using a modified Bromhead ring shear apparatus designed by Merchán (2011). Ring shear tests were performed on specimens prepared at different target water contents and statically compacted. The test results were compared with previous tests on unsaturated Boom Clay which had been prepared at higher water content and dried to the target suction. The results used to define an effective stress, which includes the influence of microstructure, to predict the residual shear strength of compacted Boom Clay.

4.1. Microstructure of compacted clays

The microstructural aspect of clay was investigated using mercury intrusion porosimetry on compacted samples of Boom Clay. The results were compared with the MIP tests performed by Merchán (2011) and Romero (1999) on compacted and remolded samples of Boom Clay. Also electron scanning environmental microphotography done by Merchán (2011) was used to evaluate the microstructural evolution of remolded samples of Boom Clay during a drying process.

Compacted samples on the dry side presented a clear bimodal distribution of porosity in the PSD curve as is expected. A large amount of inter-aggregate porosity was observed when the intra-aggregate pores were in unsaturated states. Also the amount of microporostiy was observed not to vary with the density of the sample. The gravimetric water content corresponding to a saturated microstructure was determined to be w= 10%-15%. The microporosity void ratio remains constant when intra-aggregate pores are unsaturated, and increases proportionally once saturation has been reached.

Remolded samples were found to have a monomodal PDS distribution, but upon inspection of SEM photomicrographs slight aggregation could be observed and the presence of macro and microporosity. When remolded samples are subjected to drying, the monomodal pore size distribution remains, but aggregation is also present. The main difference between the microstructure of compacted samples and dried remolded samples is the amount of macroporosity present and the size of aggregates formed. Aggregates in dried remolded samples appear to be fused together creating a more rigid structure when compared with a compacted sample in the same state.

4.2. Shear Strength of compacted unsaturated Boom Clay at very large strain

The study of shear strength behavior was carried out using statically compacted samples of Boom Clay that were prepared at target water contents to represent a range of high total suctions. The size of the clay aggregates formed was controlled through sieving to be a maximum of 2 mm in diameter. Specimens were sheared using a modified Bromhead ring shear apparatus designed by Merchán (2011) and multistage tests were executed with net normal stresses of 50, 100, and 200 kPa. The shear rate employed was 0.089 mm/min which maintains a stable stress ratio for samples in saturated and dry states.

The test results showed an increase in residual shear strength that appeared to be controlled by the increase in suction. However the increase in shear strength observed was minimal compared to the vast increase that was observed by Merchán (2011). The results confirmed the conclusion of Merchán that stated that high suction produced an increase in residual internal friction angle and not apparent cohesion as had been traditionally accepted.

The results concluded that dry density does not affect the residual shear strength. However in light of the results compared to Merchán's results it is concluded that shear stress of the soil is dependent on suction history, initial water content and on soil structure. Furthermore it was observed that the drying process stiffens the soil causing dilatant behavior, whereas a soil prepared and compacted at a specific suction does not present significant stiffness increase.

An effective stress concept based on microstructural features was used to interpret the test results. The effective stress was divided into the effective stress of the macrostructure and the microstructure. The effective stress of at the macro level was determined to be the same as the effective stress for saturated soils. The shear strength of unsaturated clay is affected mostly by intra-aggregate governing suction. It was observed in this study that samples statically compacted and not subjected to suction change, had saturated shear strength behavior when the microstructure was saturated. For this reason a degree of saturation for the microstructure S_{rm}, which does not vary with soil density, was defined and used in the definition of the microstructure effective stress.

A shear stress parameter α was defined to proportion the influence the micro effective stress has on the total effective stress. The parameter is a function of net normal stress, stress history and aggregate size. It was found that net normal stress during the application of suction greatly influenced the residual shear strength of Boom Clay. Clay specimens subjected to a drying or wetting process after compaction form bigger aggregates that behave more like granular materials than smaller aggregates. Also net normal stress during the formation of aggregates produce a fusion of aggregates further increasing the stiffness of the soil.

Finally an effective stress model for determining unsaturated residual shear strength was proposed. The model was verified with the test results from this study and from previous studies, and a very good agreement between the experimental and predicted residual shear strength was found. The model incorporates saturated shear strength parameters with suction and microstructural aspects to predict the unsaturated shear strength behavior of Boom Clay.

4.3. Future Work

This study showed the influence of suction and microstructural features on the residual shear strength behavior of unsaturated clays. However a more in depth study is needed on the following subjects.

- The influence of initial water content on the size of aggregates formed when clay is subjected to drying or wetting during the imposition of suction.
- The influence of net normal stress on the interaction of aggregates formed during drying and wetting.
- In depth study of the relationship with the shear parameter α proposed in this study, with the microstructural properties of the material.

References

Al-Homoud, A.S., Basma, A. A., Husein Malkawi, A. I., Al Bashabsheh, A. (1995) Cyclic Swelling Behavior of Clays. *Journal of Geotechnical Engineering*, July 1995, pp. 562-565.

Alonso, E. E., Pinyol, N. M., Gens, A. (2013). Compacted soil behavior: initial state, structure and constitutive modelling. *Géotechnique*, 63, No. 6, pp. 463-478.

Alonso, E. E., Pereira, J. M., Vaunat, J., Olivella, S. (2010). A microstructurally based effective stress for unsaturated soils. *Géotechnique*, 60, No. 12, pp. 913-925.

Bernier, F., Volckaert, G., Alonso, E., Villar, M. (1997). Suction-controlled experiments on Boom clay. Engineering Geology, 47, pp. 325-338.

Bishop, A. W. (1959). The principle of effective stress. *Teknisk Ukeblad*, 106, 39, pp. 859-863.

Delage, P., Le, T. T., Tang, A. M., Cui, Y. J., Li, X. L. (2007) Suction effects in Deep Boom Clay block samples. *Géotechnique*, 57, No. 1, pp. 239-244.

Della Vecchia, G., Jommi, C., Romero, E. (2012). A fully couple elastic-plastic hydromechanical model for compacted soils accounting for clay activity. *International journal for numeral and analytical methods in geomechanics.*

Deng, Y. F., Tang, A. M., Cui, Y. J., Nguyen, X. P., Li, X. L., Wounter, L. (2011). Laboratory hydro-mechanical charaterisatrion of Boom Clay at Essen Mol. *Physics and Chemistry of the Earth*, 36, pp. 1878-1890.

Farulla, C. A., Ferrari, A., Romero, E. (2010). Volume change behaviour of compacted scaly clay during cyclic suction changes. *Canadian Geotechnical Journal*, 47, pp. 688-703.

Fredlund, D. G., Morgenstern, N. R. (1977). Stress State Variables for Unsaturated Soils. *Journal of the Geotechnical Engineering Division*, 107(GTS), pp. 447-466.

Fredlund, D.G., Morgenstern, N. R., Widger, R. A. (1978). The shear strength of unsaturated soils. *Canadian Geotechnical Journal*, Vol 15, 3, pp. 313-321

Gan, J. K. M., Fredlund, D. G., Rahardjo, H. (1988). Determination of the shear strength parameters of an unsaturated soil using the direct shear test. *Canadian Geotechnical Journal*, 25, pp. 500-510.

Gens A, Alonso EE (1992). A framework for the behaviour of unsaturated expansive clays. *Canadian Geotechnical. Journal*, 29, pp. 1013–1032.

Griffiths, F. J., Joshi, R. C. (1989). Change in pore size distribution due to consolidation of clays. *Géotechnique*, 39, No. 1, pp. 159-167.

Guggenheim, S, Martin, R.T. (1995). Definition of clay and clay mineral; joint report of the AIPEA nomenclature and CMS nomenclature committees. *Clays Clay. Mineralogy*, 43, pp. 255-6

Horseman, S.T., Winter, M.G. and Entwistle, D.C. (1987). Geotechnical characterization of Boom Clay in relation to the disposal of radioactive waste. *Commission of the European Communities*.

Hueckel, T. A. (1992). Water-mineral interaction in hygromechanics of clays exposed to environmental loads: a mixture-theory approach. *Canadian Geotechnical Journal*, 29, pp. 1071-1086.

Infante Sedano, J. A., Vanapalli, S. K., Garga, V. K. (2007). Modified Ring Shear Apparatus for Unsaturated Soils Testing. *Geotechnical Testing Journal*, Vol. 30, No. 1, pp. 39-47.

Lloret, A., Villar, M. V., Sanchez, M., Gens, A., Pintado, X. & Alonso, E. E. (2003). Mechanical behaviour of heavily compacted bentonite under high suction changes. *Géotechnique* 53, No. 1, pp. 27-40

Leong, E. C., Rahardjo, H., Fredlund, D. G. (2001), Application of unsaturated soil mechanics in geotechnical engineering. *Proceedings of the 8th East Asian Pacific Conference on Structural Engineering and Construction*, Singapore, Dec. 5-7.

Khalili, N., and Khabbaz, M. H. (1998). A unique relationship for χ form the determination of shear strength of unsaturated soils. Géotechnique,48, No 5, pp. 681–688.

Koliji, A., Vulliet, L., Laloui, L. (2010) Structural characterization of unsaturated aggregated soil. *Canadian Geotechnical Journal*. 47, pp. 297-311.

Luckham, P. F., Rossi, S. (1999). The colloidal and rheological properties of bentonite suspensions. *Advances in Colloid and Interface Science*, 82, pp. 43-92.

Merchán, V., 2011. Small strain stiffness and residual strength of unsaturated Boom clay: a microstructural insight. (PhD Thesis) Universitat Politècnica de Catalunya, Barcelona, Spain.

Romero, E. (1999). Characterisation and thermo-hydro-mechanical behavior of unsaturated Boom Clay: An experimental study. (PhD Thesis) Universitat Politècnica de Catalunya, Barcelona, Spain

Romero, E., Gens, A., Lloret, A. (1999). Water permeability, wáter retention and microstructure of unsaturated compacted Boom clay. *Engineering Geology*, 54, pp. 117-127.

Romero, E., Della Vecchia, G., Jommi, C. (2011). An insight into the water retention properties of compacted clayey soils. *Géotechnique*, 61, No. 4, pp. 313-328.

Romero, E., Simms, P. H. (2008). Microstructure investigation in unsaturated soils: A review with special attention to contribution of mercury intrusión porosimetry and environmental scaning electron microscopy. *Geotechnical Geological Engineering*, 26, pp. 705-727.

Romero, E. (2011). Microstructural aspects of compacted clayey soils: An experimental viewpoint. *VII Sompósio Brasileiro de Solos Não Saturados*, Pirenópolis, GO

Saiyouri, N., Hicher, P. Y., Tessier, D. (2000). Microstructural approach and water modelling in highly compacted unsaturated swelling clays. *Mechanics of Cohesive-Frictional Materials*, 5, pp. 41-60.

Simms, P. H., Yanful, E. K. (2004). A discussion of the application of mercury intrusion porosimetry for the investigation of soils, including and evaluation of its use to estimate volume change in compacted clayey soils. *Géotechnique*, 54, No. 6, pp. 421-426.

Stark, T. D., Eid, H. T. (1994). Drained residual strength of cohesive soils. Journal of Geotechnical Engineering, Vol. 120, No. 5, pp. 856-871.

Tarantino, A., De Col, E. (2008) Compaction behaviour of clay. *Géotechnique* 58, No. 3, pp. 199-213.

Tarantino, A. (2011). Unsaturated soils: Compacted versus reconstituted states. *Proceedings of the 5th International Conference on Unsaturated Soils*, Barcelona, Vol. 1, pp. 113-136.

Terzaghi K.(1936).The shearing resistance of saturated soils and the angle between the planes of shear. *International Conference on Soil Mechanics and Foundation Engineering. Harvard University Press*: Cambridge, MA, pp. 54–56.

Vanapalli, S. K., Fredlund, D. G., Pufahl, D. E. (1999). The influence of soil structure and stress history on the soil-water characteristics of a compacted till. *Géotechnique*, 49, No. 2, pp. 143-159.

Velosa, C. L. (2011). Unsaturated soil behavior under large deformations using a fully servo/suction-controlled ringh shear apparatus. (PhD Tesis) University of Texas at Arlington, Arlington, USA.

Wheeler, S. J., Sivakumar, V. (2000) Influence of compaction procedure on the mechanical bahaviour of an unsaturated compacted clay, Parts 1 and 2. *Géotechnique*, Volume 50, Issue 4, 01 August 2000, pp. 259-376.

Wheeler, S. J., Sharma, R. S., Buisson, M. S. R. (2003). Coupling of hydraulic hysteresis and stress-strain behavior in unsaturated soils. *Geotechnique* 53, No. 1, pp. 41-54